Energy Mines and Resources Canada | Energie Mines et Ressources Canada

CANMET

Canada Centre for Mineral and Energy Technology | Centre canadien de la technologie des minéraux et de l'énergie

MINERALOGY OF TAILINGS FROM DELNITE MINES, A FORMER GOLD PRODUCER NEAR TIMMINS, ONTARIO

J.L. Jambor
Process Mineralogy Section
Mineral Processing Laboratory

D.W. Blowes
Waterloo Centre for Groundwater Research
University of Waterloo
Waterloo, Ontario

D.R. Owens
Process Mineralogy Section
Mineral Processing Laboratory

February 1991

Project: 30.05.03
Tailings Characterization and Treatment

MICROMEDIA

61 pp

MINERAL SCIENCES LABORATORIES
DIVISION REPORT MSL 91-26(IR)

This document is an unedited interim report prepared primarily for circulation and internal reporting purposes. It does not represent a final expression of the opinion of the Canada Centre for Mineral and Energy Technology (CANMET)

Ce document est un rapport provisoire non-révisé et rédigé d'un document pour fin de diffusion et de documentation interne. Il ne représente nullement l'expression définitive de l'opinion du Centre canadien de la technologie des minéraux et de l'énergie (CANMET)

MINERALOGY OF TAILINGS FROM DELNITE MINES, A FORMER GOLD PRODUCER NEAR TIMMINS, ONTARIO

by

J.L. Jambor, D.W. Blowes, and D.R. Owens

ABSTRACT

The Delnite mine near Timmins, Ontario, processed approximately 3.5 million tonnes of gold ore during its 27-year lifespan to closure in 1964. The gold occurred in carbonate-rich quartz veins containing 3-5 wt% sulphides consisting mainly of pyrite with lesser amounts of pyrrhotite and small amounts of arsenopyrite. Oxidation of the tailings, which were deposited in a 25-ha impoundment elevated 3-10 m above the surrounding land, has discoloured only the uppermost 60-100 cm, wherein the partial alteration of sulphides indicates that pyrrhotite has been the most susceptible to attack. Electron-microprobe analyses have shown that alteration rims on sulphides are highly variable in composition; the rims contain up to 18.7 wt% As_2O_5, and up to 2.6 wt% SiO_2, 3.9% CaO, and 10.0 wt% SO_3. X-ray powder-diffraction patterns indicate that the rims consist of goethite. No crystalline arsenate mineral was detected. The acid generated by oxidation of the sulphides is buffered by reaction with the carbonate-rich components of the tailings, thereby releasing Ca^{++} to form gypsum. Reconnaissance analyses of waters within the tailings gave values up to 6.2 mg/L for total cyanide. The highest

concentrations of cyanide occur in the impoundment in an area that was concluded by other studies to have retained the highest proportion of undiluted mill process-water. The other studies also indicated that the arsenic released by the breakdown of sulphides may be moving unretarded through the tailings.

Keywords: tailings, sulphides, carbonates, oxidation, goethite, arsenic, cyanide, Delnite minesite, Timmins, Ontario

INTRODUCTION

The Delnite minesite is in Deloro Township, about 5 km south of Timmins, Ontario. The mine is within the geological framework of the Porcupine gold camp, which includes world-renowned producers such as the Hollinger, McIntyre, and Dome mines (Fig. 1). The Delnite mine was a modest producer relative to these giants, and during its lifetime from 1937 to 1964 the mill processed approximately 3,490,000 tonnes of ore grading 6.22 g Au/t (0.20 oz/ton) (Ferguson et al., 1971). During 1987-1988 a small amount of high-grade ore (~53,500 tonnes grading 29.3 g Au/t) was produced by open pit (Luhta et al., 1990). Delnite is among the group of several sites in the Timmins area whose combined total of 137 million tonnes of gold-bearing tailings will be re-milled for additional gold recovery (Luhta et al., 1989, 1990).

The Delnite site was selected for study (Blowes, 1990) in part so that the effects of sulphide oxidation in a carbonate-rich tailings environment could be compared with the effects that have been described for the sulphide-poor, carbonate-depleted environment of the Nordic Main uranium-tailings impoundment at Elliot Lake (Blair, 1981; Blair et al., 1980; Cherry et al., 1980; Dubrovsky, 1986; Dubrovsky et al., 1984). The Delnite tailings were also selected for study because the arsenopyrite in the ore was discharged as a component of the tailings. The Delnite site, therefore, provided an opportunity to study the behaviour of arsenic in a carbonate-buffered geochemical system. An initial

report on the mineralogy of Delnite cores from site D1 was presented by Jambor & Blowes (1991). The present study is a more complete record of the results from D1, and also presents data for a second site, D5.

Site Description

The gold ore at the Delnite mine occurred (Stevens, 1944; Taylor, 1948) as two generations of veins hosted by light-grey, highly carbonatized andesitic pillow flows. The older generation of veins, which was referred to as "grey veins", consisted of grey, cherty quartz, dolomite (so-called ankerite), and later glassy quartz accompanied by smaller amounts of mica (so-called fuchsite and sericite) and traces of scheelite. Sulphide minerals associated with the grey veins were pyrite and arsenopyrite. The younger generation of veins, which was referred to as "brown veins", occurred in greater tonnage and generally had a higher grade of Au. The brown veins consisted of dolomite (ankerite), glassy quartz, massive brown tourmaline, and minor amounts of calcite and scheelite. The most abundant sulphides associated with the brown veins were pyrite and arsenopyrite, with chalcopyrite, sphalerite, and pyrrhotite rarely present in minor amounts. The gold in both sets of veins was primarily associated with the pyrite and arsenopyrite; Stevens (1944) reported observations of native gold in grains ranging from <6 μm to 50 μm. Gold grains in pyrite occurred as inclusions, whereas gold grains in arsenopyrite were along fractures, with or without chalcopyrite. Later reports of

the ore (Stevens 1964) indicated the gold to be intimately associated with pyrrhotite.

Mill production at Delnite commenced June 1, 1937, and ended in 1964 (Stevens 1964). The Delnite mill was initially designed for a straight cyanide-extraction process, but gold recoveries averaged only about 92%. In 1941 the mill was converted to a flotation-cyanide process to enhance recoveries; although the improvement initially was only to about 93%, in 1963 and 1964 the recoveries were apparently about 94.5% (Stevens 1964). The initial production at approximately 180 tonnes/day (200 tons/day) was increased to approximately 450 tonnes/day (500 tons/day) in 1944, and remained at that rate until mill closure in 1964.

Throughout production, the tailings were deposited in a depression immediately adjacent to the mill. These tailings eventually accumulated into an elevated 25-ha impoundment (Figs. 2,3) which stands 3-10 m above the surrounding terrain. The impoundment was decommissioned in 1964, and the surface was revegetated in 1971 through the addition of limestone and fertilizer. The impoundment is grass-covered and has a relatively flat top; there is little surface runoff, and the general direction of groundwater movement is downward. The tailings are underlain by a discontinuous peat and clay layer that ranges from >2 m thick at piezometer nest D1 at the eastern end of the impoundment (Fig. 2), to <0.10 m thick at D17 in the center of the impoundment, and to absent at D13 at the western end of the impoundment. Beneath the peat/clay layer is a fine-grained sand aquifer that is <2 to >6 m

thick. The sand unit is underlain by a blue-grey till; exposures in an open pit near the tailings indicate that the till directly overlies the irregular bedrock surface.

Surface water originating in the Delnite impoundment is collected in drainage channels along the southern, western, and eastern margins of the impoundment. Drainage enters a small creek, which is a tributary of the South Porcupine River, and ultimately drains into Porcupine Lake 8 km from the impoundment. Water quality in the drainage channels and in the creek is monitored on a regular basis; no occurrence of poor-quality drainage has been reported.

Tailings solids

The tailings were cored in sections about 1 m long and 7.6 cm (3 in.) in diameter (Blowes 1990). The core was cut into 20-cm sections, was frozen at the field site, and was shipped and stored frozen at Waterloo until ready for study. Cores from Delnite holes D1 and D5 have been mineralogically examined at CANMET. Prior to shipment to CANMET, the cores were sawn along their length so that half could be retained at Waterloo. The other half, still in its aluminum-pipe core-barrel, was bagged in plastic, packed in an insulated container, and was shipped by courier to Ottawa. The orientation of each piece of core had been marked on its barrel, and each sample had been assigned a number that increased with the down-hole progression; the cores received for both Delnite hole D1 and hole D5 are C1 to C10, inclusive, and C12. Each core piece was

about 20 cm long, the exception being D1-C12, which measured 29 cm in length. The total depth for each borehole series, therefore, is approximately 2.5 m.

Tailings waters

The groundwater-flow system within the tailings and in the underlying and adjoining Pleistocene deposits was determined and reported by Blowes (1990). The chemical compositions of the tailings pore water and pore gas were determined in detail by Blowes (1990) for 8 piezometer nests on the impoundment, and for survey samples at 24 more sites in and around the impoundment. Although the present study is concerned almost exclusively with the tailings solids, a reconnaissance sampling of the tailings waters was conducted to establish whether their total cyanide contents were significant.

RESULTS

The cores as received were in good condition and had remained frozen. As in previous studies (Blowes & Jambor 1990; Jambor & Blowes 1989, 1991) the wrapping material and aluminum core-barrel containers were discarded after ejection of the frozen cores into labelled, plastic-lined boxes. Thawing and drying of the cores took place under normal, room-temperature conditions; the progression to dryness was uneventful, and no significant sulphate blooms or fracture patterns were developed. The absence of

sulphate blooms presumably reflects the low sulphide content of the Delnite tailings.

The megascopic character of the cores from holes D1 and D5 are given in Tables 1 and 2, respectively. For the most part the tailings are fine-grained to the extent that they are typically clay-like rather than sandy or silty. The most significant variation is that the first three near-surface cores in each hole are ochreous, whereas all others are grey. This suggests that only the uppermost 0.6 m of the tailings at the D1 and D5 sites have been appreciably oxidized.

Microscopic examination

Portions of the almost dry cores were removed with a utility-blade knife by cutting successive slices along the axis of elongation. The material removed in this way generally amounted to a third or half of the core, and the remainder was kept intact. The removed slices were screened to minus 270 mesh (aperture size 53 μm), and a portion of the powder from each sample was mounted in polished section. For hole D1, cores C6 to C12 were not subdivided, but cores C2 to C5, inclusive, were each divided into top and bottom halves (uphole half and downhole half, respectively); core C1 also was subsampled, but as top, middle, and bottom portions. The total number of samples and polished sections, therefore, was seventeen. For hole D5, all of the cores were divided into top and bottom halves (except C4, which was split into three sections), and the result was twenty-three samples. The combined total from both holes amounted to fifty polished sections.

Study of polished sections by reflected-light microscopy showed that grain sizes of the sulphides vary substantially from sample to sample; maximum sizes are about 30 x 60 μm, and more than 95% of the sulphide grains are less than 25 x 30 μm. The volume of sulphides in the samples was estimated visually to be 2-4%, and the wt.% sulphides is therefore inferred to be about 3-5%. The sparseness of the sulphide grains, and their small size on average, combine to give the misleading impression that the ore was exceedingly fine-grained. In several polished sections, however, it was noted that many of the silicate and carbonate grains are several times coarser than the accompanying sulphides. This substantial difference in grain sizes is probably a consequence of the Delnite milling procedure; according to Stevens (1944) the ore was crushed to 50-58% minus 200 mesh (aperture size 75 μm), followed by separation of the sulphide fraction by differential flotation. The sulphide concentrate was then reground to minus 325 mesh (aperture size 49 μm) prior to cyanidation. The coarse flotation tails and the cyanide-treated sulphide tails were combined and discharged to the impoundment. The fine grain size of the sulphide particles thus is mainly a consequence of the procedures that were used to liberate the gold.

The principal sulphides observed are pyrite and minor pyrrhotite. Minute amounts of arsenopyrite are present in nearly all samples, and trace amounts of chalcopyrite occur erratically; one grain of chalcopyrite was observed to contain a minute inclusion of a Co-Fe-As sulphide, possibly glaucodot. In both

holes the sample from nearest the surface (sample C1T) has a negligible pyrrhotite content, and nearly all sulphide grains have non-sulphide alteration rims. Likewise in both holes, residual grains of alteration-rimmed pyrrhotite appear in small amounts in sample C1B.

For drillhole D1, the decrease in alteration below sample C1 seems to be progressive: in the underlying sample (C2), a slight weakening of alteration is indicated by a narrowing in the width of the rims, by the presence of many grains whose edges are irregularly corroded but not rimmed, and by the presence of a few negligibly altered grains. Sample C3 shows a further weakening of alteration; by the middle of sample C4 the edges of all or nearly all sulphide grains, including pyrrhotite, are sharp and unaltered. These results are in good agreement with the depth of oxidation inferred from the megascopic changes in color from ochrous near the surface to grey at depth (Table 1).

For drillhole D5, the decrease in alteration below sample C1, although more variable in detail, was similar to that in D1. In D5, residual pyrrhotite first appears in sample C1B, and alteration rinds extend from the top of the hole to the top of core C4. The top part of C4 (excluding the 1.5-cm ochrous zone -- Table 2) shows notably fewer alteration rims, and by the bottom of C4 the sulphides are unaltered.

X-ray diffractometry

Attempts were made to obtain mineral separates by using heavy

liquids, isodynamic magnetic separation, and selective dissolution with weak acids. The first two methods were totally ineffective because of the fine grain size of the tailings, but treatment with 5% HCl indicated that major amounts of dolomite and small amounts of siderite are present even in the near-surface sample (Fig. 4).

Diffractograms of cores C1, C2 and C3 from hole D1 are shown in Figure 5; these samples are from the oxidized near-surface zone, whereas cores C4M to C10 (Fig. 6) are unoxidized, deeper samples. All samples contain chlorite, muscovite, quartz, albite, dolomite, and tourmaline as their principal constituents. In addition to dolomite, all samples contain small amounts of siderite; no calcite, however, is evident in the X-ray patterns. Only two major differences distinguish the two sets of samples: (1) gypsum is detectable in the near-surface samples, attaining maximum abundances near the bottom of the oxidized zone; (2) talc is present only in the unoxidized cores, and is abundant only in the three deepest samples (Fig. 6).

Diffractograms of samples from hole D5 are shown in Figures 7, 8 and 9. As for D1, gypsum is detectable near the top of the hole, and talc appears only in the lower samples. Siderite and dolomite contents are variable from core to core but, as shown in Figure 9, the uppermost samples (C1T and C1B) do have low amounts of carbonate. This low content could be the result of carbonate dissolution, or simply may reflect a low carbonate content in the initial, "primary" tailings.

The mineral variations noted above are attributed to two completely different origins. Taylor (1948) reported that almost all of the ore mined at Delnite was in carbonatized andesite, and almost all of the andesite was sandwiched between talc-chlorite schist. According to Stevens (1944), the extremities of some veins extended into the schist, and "To obtain all the ore it has, at times, been necessary to mine the ends of these veins which have entered the chlorite schist. It is found that the inclusion of chlorite schist in the mill feed tends to affect adversely the efficiency of the flotation" (Stevens 1944, p. 501). It seems likely, therefore, that in the later years of operation the ends of the veins either were not extracted, or the mining methods were improved sufficiently to avoid significant dilution by the talc-chlorite schist. For drillhole D1, which was the only core examined by Jambor and Blowes (1991), the disappearance of talc in the stratigraphically younger tailings coincides with the appearance of the zone of oxidation. Despite this coincidence in D1, talc in D5 first appears substantially below the depth of the oxidized zone (Figs. 7,8); this observation confirms the previous conclusion (Jambor & Blowes 1991) that the occurrence of talc is unrelated to the position of the oxidized zone.

In contrast to the primary origin assigned to talc, a secondary origin for the high concentrations of gypsum in the oxidation zone is readily attributable to processes involving the alteration of sulphides within the tailings solids. Oxidation of pyrite, pyrrhotite, and arsenopyrite generates sulphate-rich acidic

solutions that attack the associated dolomite, thereby releasing Ca^{2+} (as well as Mg^{2+} and some Fe^{2+}) that combines with available sulphate to form the gypsum. Within the oxidized zone in hole D1, the trend from relatively low amounts of gypsum nearest the surface, to highest amounts near the bottom of the oxidized zone (Figs. 5, 6), is likely an indication that near-surface gypsum is being dissolved and is being reprecipitated deeper in the oxide zone. For hole D5, gypsum abundance appears to highest in the middle of the oxidized zone (Figs. 7, 9).

In addition to the X-ray diffractograms of the bulk samples of tailings solids, individual grains were examined by Debye-Scherrer X-ray film techniques, and by scanning electron microscopy combined with energy-dispersion (SEM-EDX) analyses. As was mentioned previously, precipitates that typically form as abundant efflorescences during the drying of sulphide-rich cores (e.g., Jambor & Blowes 1989) are notably sparse on the Delnite cores; these secondary precipitates were observed only on cores from below the oxidized zone, seemingly most abundantly on C5 and the upper part of C6 of borehole D1. Almost all of the precipitate is gypsum, which occurs in mm-size local patches and as disseminated, grey, pinhead-size aggregates. Some of the aggregates have aureoles of white hexahydrite ($MgSO_4.6H_2O$) that also occurs locally as clear coatings (Fig. 10). In addition to gypsum and hexahydrite, a few spheres (Fig. 11) were observed of a phase for which only S ± Cl could be detected by EDX. The S-rich spheres may be native sulphur, but unlike hexahydrite, no confirmation by X-ray diffraction could be obtained.

Electron-microprobe analyses

Electron-microprobe analyses of the tailings carbonates were done to establish the general range of compositions of the dolomite and siderite. The results (Table 3) indicate that dolomite is consistently iron-rich, and that the associated siderite is consistently highly magnesium-rich; one of the 21 grains analyzed is ferroan magnesite. All grains contain manganese, with the maximum wt% MnO in dolomite approximating the minimum MnO of siderite; the respective averages are 0.43 and 0.73 wt% MnO. Microprobe analyses for Zn, Sr, and Ba as possible solid-solution components of the carbonates gave negative results.

SEM photographs and corresponding element X-ray maps for altered sulphide grains are shown in Figures 12 to 23, and quantitative electron-microprobe analyses for specific areas within the Figures are given in Table 4. All of the analyses show that the alteration rims contain at least 60 wt% Fe as Fe_2O_3, and the variation is up to 78.8 wt% Fe_2O_3. Other elements, namely Ca, Si, As, and S, are present in relatively small and highly variable amounts: the wt% range for CaO is 0.0 - 3.4, and that for SiO_2 is 0.9-2.6. Although the X-ray maps indicate that Ca and Si in many of the rims are homogeneously distributed, the combination of high Fe values with low Ca and Si indicates that the latter two are present as solid-solution components or, more probable, as physical admixtures. The remaining two elements, namely As and S, are typically assumed to be present as AsO_4 and SO_4, though in any specific analysis there is always concern of enhancement by

fluorescence effects from the adjoining precursor sulphide. Table 4 shows, nevertheless, that in 14 of the 18 analyses the amount of total S as SO_4 is <4.2 wt%; as was suggested for Ca and Si, it seems likely that such low SO_4 values represent a solid-solution component or physically admixed phase. The highest SO_4 value coincides with the highest Fe_2O_3 percentage, and the ratio $Fe:(SO_4,AsO_4,SiO_4)$ is about 5:1. No mineral with such a ratio is known, and the closest in composition is so-called "glockerite", which has been shown to be a sulphate-bearing or sulphate-contaminated goethite.

Arsenic contents of the alteration rims range from 1.9 to 22.6 wt% AsO_4, and average 10.3%. The analysis with the highest AsO_4 value was obtained from a narrow rim on arsenopyrite (Fig. 17), so arsenic enhancement because of fluorescence is a distinct possibility; the analysis leads to a formula approximating $Fe_4^{3+}(AsO_4)(OH)_{10}$, but no mineral with this composition is known. The other analyses that are rich in arsenic give similarly high or higher Fe:As ratios, beyond those known for minerals.

Attempts were made to make X-ray mounts of the alteration rims while observing them under a metallographic microscope. Because of the small size of the grains, the efforts were unsuccessful; only the residual sulphide cores were identifiable on the X-ray patterns. Numerous individual grains hand-picked under a binocular microscope gave X-ray patterns consistently indicating that goethite is the only crystalline alteration product associated with the sulphides, and no arsenates were detected.

The results obtained from the microprobe analyses and X-ray patterns are interpreted as indicating that almost all of the material in the alteration rims is goethite. The nature of the Ca, Si, As, and "SO_4" is, however, less certain; structural incorporation of silicon and various unusual cations in goethite has been reported by numerous authors (e.g., Schwertmann & Taylor 1972; Quinn et al. 1988; Bobkovskii & Yalovoi 1987; Gerth 1990); nevertheless, the adsorption of elements, including the adsorption of anions, also is widely known for goethite and various iron hydroxides (e.g., Hingston et al. 1974; Russell et al. 1975; Balistrieri & Murray 1982; Parfitt et al. 1975; Harrison & Berkheiser 1982; Yapp 1987). Although the quality of the X-ray patterns of the Delnite goethite is not high, the results are adequate to indicate that a major substitution of other elements has not occurred; because of this observation, and the tenor and variations in compositions of the rims, it is inferred that adsorption rather than solid solution has been the principal mechanism of incorporating the additional elements with goethite. It is possible that the rims with the highest values in AsO_4 contain a discrete arsenate phase, but the arsenate may be amorphous to poorly crystalline and variable in composition, as is commonly found for arseniosiderite, ideally $Ca_3Fe_4(AsO_4)_4(OH)_6.3H_2O$. The iron arsenate most likely to be present is $Fe(AsO_4).2H_2O$ (scorodite); less likely because of the high As:Fe ratio is $Fe_3(AsO_4)_2.8H_2O$ (symplesite).

In contrast to arsenic, it is probable that even the highest values for SO_4-equivalent do not represent a discrete *sulphate* phase. A peculiarity in some of the rims is that the sulphur detected by electron microprobe is at the wavelength position characteristic of sulphide sulphur rather than sulphate sulphur. Among the possible explanations for this phenomenon are (a) the presence of submicroscopic inclusions of residual sulphides; (b) fluorescence effects from adjacent grains; (c) wavelength shifts related to absorption, as distinct from crystal-structural bonding, and (d) the presence of native sulphur, rather than sulphide or sulphate. The first two possibilities (inclusions and fluorescence) are not consistent with the microscopic observations and analytical results, especially where a "shrinking core" model of alteration appears to be appropriate for most of the grains. The possibility of a wavelength shift (c) is not only unlikely, but has not been observed or reported to occur elsewhere. The presence of native sulphur derived by alteration of sulphides, and which is associated with other alteration products, is well known. Although sulphur at Delnite has not been confirmed by X-ray diffraction study, its presence in the alteration rims is thought to offer the best explanation for the electron-microprobe results.

CYANIDE ANALYSES

In mid-November of 1990, several samples of Delnite tailings pore waters were collected to determine the possible presence of

residual cyanide. The samples were frozen at the field site and were kept frozen until a few days prior to analysis for total cyanide by the Chemical Laboratory of CANMET. As no other precautions had been taken, such as stabilization of the solutions by means of Na(OH), some degradation of the cyanide may have occurred.

The results of the analyses (Table 5) showed that cyanide levels are much higher than anticipated; low or background values were the expectation because cyanide is readily susceptible to natural degradation, and the treatment of ore at Delnite ceased more than 25 years prior to the sampling. The significance of the high values of 6.2 and 6.0 mg/L can be judged in the light of environmental regulations: the U.S. Environmental Protection Agency has proposed recently (July, 1990) a drinking-water standard of 0.2 mg/L cyanide (Rouse 1990). The maximum legally permissible cyanide level in South Africa is 0.5 mg/L (Mining Journal, 1990), and the recommended "Guideline Value" of the Ontario Ministry of Environment is 2.0 mg/L.

The lowest cyanide values at Delnite were obtained from piezometer sites D1 and D3, and the highest values were obtained from site D17 (Fig. 2; Table 5). On the basis of ^{3}H concentrations in the tailings waters, Blowes (1990) concluded that mill process-waters, which were discharged into the impoundment with the tailings, are concentrated in the area of piezometer nests D13 and D17 (Fig. 2). Thus, the highest cyanide values coincide with the apparent occurrence of the least diluted mill process-waters.

CONCLUSIONS

The principal reactant minerals in the Delnite tailings are pyrrhotite, arsenopyrite, and pyrite. The least stable sulphide is pyrrhotite, which is much more extensively altered than pyrite and arsenopyrite. As the widths of alteration rims around pyrite and arsenopyrite are similar, presumable these minerals are equally stable in the tailings environment. The mineralogical variations indicate that alteration of sulphides is limited to the uppermost 60 cm of the tailings. Chemical analyses of the bulk solids in this oxidized zone show an apparent depletion in carbonates, and possibly in sulphides (Fig. 24). Attack of the carbonates by acid generated from the observed partial alteration of sulphides would account for a depletion in carbonate solids, and for the near-neutral pH of the tailings waters (Blowes 1990).

The presence of carbonate in solution is known to favour the precipitation of goethite (Ross & Wang 1982; Carlson & Schwertman 1990), and most of the iron released by destruction of the sulphides seems to have been deposited as goethite. Substantial amounts of calcium and magnesium, as well as additional iron, are released by carbonate dissolution. The mineralogical studies indicate that the calcium combines with the sulphide-derived sulphate to form gypsum, and that the magnesium stays in solution rather than forming a secondary solid. Arsenic, which is derived from the dissolution of pyrite as well as arsenopyrite, is precipitated mainly with the goethite, probably at least in part as

an iron arsenate solid phase. Blowes (1990) reported that concentrations of total arsenic in pore waters (max. = 25 mg/L) are low near the tailings surface; arsenic concentrations and those of Fe^{2+} increase abruptly at approximately the same depth, thereby suggesting that both are released by sulphide oxidation. At some sites, however, the maximum arsenic concentrations exceed those of iron, and at depth the "leading edge" of the high arsenic values occurs deeper in the tailings than that of Fe. These observations suggest that arsenic is passing unretarded through the tailings and into the surrounding groundwater system. Nevertheless, Blowes (1990) reported that analyses of three water samples from seepage faces at the perimeter of the impoundment gave arsenic values of <10 µg/L to >2 mg/L. Arsenic concentrations in the waters of the drainage channel adjacent to the tailings are consistently <10 µg/L, and these values do not indicate a need for environmental concern. In time, however, the water quality may decline as the front of higher arsenic concentrations gradually moves through the impoundment. As well, the results of the reconnaissance study of total cyanide in the pore waters similarly indicate that cyanide may pose an environmental problem unless there is future dilution of the residual mill process-waters. Additional sampling is being undertaken to define more clearly the pattern for cyanide distribution and abundance, and their relationships to present and future movements of waters through the Delnite impoundment.

ACKNOWLEDGMENTS

Technical assistance at CANMET was kindly provided by P. Carrière (X-ray), and J.M. Greer (lapidary).

REFERENCES

Balistrieri, L.S. and Murray, J.W. (1982): The adsorption of Cu, Pb, Zn, and Cd on goethite from major ion seawater. Geochim. Cosmochim. Acta **46**, 1253-1265.

Blair, R.D. (1981): Hydrogeochemistry of an Inactive Pyritic *Tailings Impoundment Tailings Basis, Nordic Mine, Elliot Lake, Ontario*. M.Sc. thesis, University of Waterloo, Waterloo, Ontario.

Blair, R.D., Cherry, J.A., Lim, T.P. and Vivyurka, A.J. (1980): Groundwater monitoring and contaminant occurrence at an abandoned tailings area, Elliot Lake, Ontario. *In*: Proc. First Internat. Conf. on Uranium Mine Waste Disposal (C. Brawner, ed.). Soc. Mining Eng., AIME.

Blowes, D.W. (1990): *The Geochemistry, Hydrogeology and Mineralogy of Decommissioned Sulfide Tailings. A Comparative Study*. Ph.D. thesis, University of Waterloo, Waterloo, Ontario, Canada.

Blowes, D.W. and Jambor, J.L. (1990): The pore-water geochemistry and the mineralogy of the vadose zone of sulfide tailings, Waite Amulet, Quebec, Canada. Applied Geochem. **5**, 327-346.

Bobkovskii, A.G. and Yalovoi, A.A. (1987): Mössbauer spectra for estimating the extent of replacement in natural goethite. Geokhimiya **1987**, (12), 1802-1806.

Carlson, L. and Schwertman, U. (1990): The effect of CO_2 and oxidation rate on the formation of goethite versus

lepidocrocite from an Fe(II) system at pH 6 and 7. Clay Minerals **25**, 65-71.

Cherry, J.A., Blackport, R.J., Dubrovsky, N.M., Gillham, R.W., Lim, T.P., Morin, K.A., Murray, D., Reardon, E.J. and Smyth, D.J.A. (1980): Subsurface hydrology and geochemical evolution of inactive pyritic tailings in the Elliot Lake Uranium District, Canada. *In*: Proceedings of the Symposium on Uranium Mill Tailings Management, Colorado State University, 353-385.

Douglas, R.J.W., ed. (1970): Geology and economic minerals of Canada. Geol. Surv. Can., Econ. Geol. Rep. **1**.

Dubrovsky, N.M. (1986): *Geochemical Evolution of Inactive Pyritic Tailings in the Elliot Lake Uranium District*. Ph.D. thesis, University of Waterloo, Waterloo, Ontario, Canada.

Dubrovsky, N.M., Cherry, J.A., Reardon, E.J. and Vivyurka, A.J. (1984): Geochemical evolution of inactive pyritic tailings in the Elliot Lake Uranium District: 1, The groundwater zone. Can. Geotech. J. **22**, 110-128.

Ferguson, S.A., Groen, H.A. and Haynes, R. (1971): Gold deposits of Ontario. Ont. Division Mines, Mineral Resources Circ. **13**.

Gerth, J. (1990): Unit-cell dimensions of pure and trace metal-associated goethites. Geochim. Cosmochim. Acta **54**, 363-371.

Harrison, J.B. and Berkheiser, V.E. (1982): Anion interactions with freshly prepared hydrous iron oxides. Clays Clay Minerals **30**, 97-102.

Hingston, F.J., Posner, A.M. and Quirk, J.P. (1974): Anion adsorption by goethite and gibbsite II. Desorption of anions

from hydrous oxide surfaces. J. Soil Sci. **25**, 16-26.

Jambor, J.L. and Blowes, D.W. (1989): Mineralogical examination of tailings from the Heath Steele mill, Newcastle area, New Brunswick. Energy, Mines and Resources, CANMET Division Report **MSL 89-137(IR)**.

Jambor, J.L. & Blowes, D.W. (1991): Mineralogical study of low-sulphide, high-carbonate, arsenic-bearing tailings from the Delnite minesite, Timmins area, Ontario. Energy, Mines and Resources, CANMET Division Report **MSL 91-17 (OP&J)**.

Luhta, L.E., Sangster, P.J., Draper, D.M., Ireland, J.C., Bradshwaw, M.P. and Hamblin, C.D. (1989): Timmins Resident Geologist's District - 1988. *In*: Report of Activities 1988, Resident Geologists, Ont. Geolog. Surv. Misc. Pap. **142**, 219-266.

Luhta, L.E., Sangster, P., Ireland, J., Hamblin, C. and Bradshaw, M. (1990): Timmins Resident Geologist's District - 1989. *In*: Report of Activities 1989, Resident Geologists. Ont. Geol. Surv. Misc. Pap. **147**, 217-254.

Mining Journal (1990): Rapid cyanide detection in effluents & tailings ponds. Mining J. (London) **315** (8088), p. 196.

Parfitt, R.L., Russell, J.D. and Farmer, V.C. (1975): Confirmation of the surface structures of goethite (α-FeOOH) and phosphated goethite by infrared spectroscopy. J. Chem. Soc. Faraday Trans. **72**, 1082-1087.

Quin, T.G., Long, G.J., Benson, C.G., Mann, S and Williams, R.J.P. (1988): Influence of silicon and phosphorus on structural and

magnetic properties of synthetic goethite and related oxides. Clays Clay Minerals **36**, 165-175.

Ross, G.J. and Wang, C. (1982): Lepidocrocite in a calcareous, well-drained soil. Clays Clay Minerals **30**, 394-396.

Rouse, J.V. (1990): Cyanide and the environment. Mining J. (London) **315** (8085, Supplement), 18-19.

Russell, J.D., Paterson, E., Fraser, A.R. and Farmer, V.C. (1975): Adsorption of carbon dioxide on goethite (α-FeOOH) surfaces, and its implications for anion adsorption. J. Chem. Soc. Faraday Trans. **71**, 1623-1630.

Schwertmann, U. and Taylor, R.M. (1972): The influence of silicate in the transformation of lepidocrocite to goethite. Clays Clay Minerals **20**, 159-164.

Stevens, C.S. (1944): Milling and metallurgy at Delnite Mines. Trans. Can. Inst. Mining Metall. **47**, 501-518.

Stevens, C.S. (1964): Automatic control of akalinity in regrind circuit at Delnite Mines Ltd. *In*: Proc. First Ann. Meet. Can. Gold Metall., Ottawa, Jan. 1964, 49-55.

Taylor, R.B. (1948): Delnite mine. *In*: Structural Geology of Canadian Ore Deposits. Can. Inst. Mining Metall. Jubilee Vol., 504-507.

Yapp, C.J. (1987): A possible goethite-iron (III) carbonate solid solution and the determination of CO_2 partial pressures in low-temperature geological systems. Chem. Geol. **64**, 259-268.

Table 1. Megascopic characteristics of Delnite core D1

C1: Light brown ochrous colour, with uppermost 2-3 cm dark, more soil-like and rich in vegetation (twigs and roots up to 1.5 mm in diameter); roots, although sparse and sporadic in occurrence, persist to the bottom of the core. Core is fine-grained (silty to clay-like rather than sandy), and much is well-bedded. Bedding is horizontal (i.e., normal to core length) except that outer (rim) part of the core is deformed into streaks resembling bedding that are parallel to the core elongation.

C2: Similar in colour to C1. Small amount of vegetation (roots) in uppermost part of sample. Parts of core show that bedding is relatively flat, but in most of the core the bedding is indistinct, and the outer part is deformed as in C1.

C3: Parts are well-laminated, showing horizontal bedding. Colour still similar to that of C1 except that some of the laminations are whiter, and such layers are finer grained than the main mass. Laminated portions are sufficiently cohesive to remain intact, whereas much of the remainder of the core is sandy and disintegrates readily. Sandy parts in the bottom third are darker than sandy parts in the upper part of the core, suggesting that oxidation effects are declining.

C4: Uppermost part of C4, which is grey and unoxidized, is drastically different from the oxidized bottom of C3; that the core may have been accidentally inverted and mislabelled is

suggested by the presence of 1-2 cm of well-oxidized, ochrous tailings in a low-angle, but distorted contact with the grey unoxidized core. Despite this contact, the main body of core shows well-defined lamination parallel to the core length, and streaks of ochrous tailings, up to 5 mm thick and 8 cm long, also occur roughly parallel to the core length. These observations indicate that severe deformation of the tailings occurred during the coring procedures. The core is fine-grained, clay-like, and more cohesive than the C1-C3 samples.

C5: More than 90% of core is grey, but again the ochrous streaks are present; the grey portion shows well-developed lamination, clearly visible as being parallel to the core length for the full length of the core. The lamination appears to be undisturbed except for minor gentle folding of the end of the core. Cores from C5 onward are cohesive and readily handled without breakage. Secondary sulphates that precipitate on the core surfaces during drying are sparse on all of the cores, but are the most conspicuous on core C5.

C6: Less well-laminated than C5, but again clearly parallel to core length. Grey, fine-grained, with ochrous material exclusively restricted as the outermost rim of the core.

C7: Similar to C6 in grey color, cohesion, fine grain size. Grain-size variations indicate that bedding is parallel to core length. Only traces (<1%) of ochrous material, all of which is restricted to the outermost 5 mm of the core.

Table 1 (cont'd)

C8: Similar to C7, but no ochrous rind. Laminated or bedded parallel to core length.

C9: Same as C8.

C10: Similar to C8 and C9, but clayey and massive except for streaking parallel to core length in the outermost rind of 0.5 cm thickness.

C12: Bottom half is clay-like and similar to the preceding (uphole) samples; streaking at outer edge of core is parallel to elongation, whereas bedding approaches horizontal towards the centre of the core. In the upper half of this core, the initial 3-4 cm of "clay" passes downward to coarser, non-cohesive, sandy tailings in which the bedding and bottom contact clearly are horizontal (perpendicular to core length).

Table 2. Megascopic characteristics of Delnite core D5

C1: Light brownish, ochrous, identical in colour to C1 in hole D1. Mud and some vegetation (twigs, roots, leaves) in uppermost 1-2 cm. Core mainly intact as cohesive lumps each about 2 cm long; poorly bedded, very fine-grained.

C2: Ochrous, but colour slightly darker and more reddish than C1 or C3; only traces of roots; more cohesive than C1, and is also coarser grained. Fairly well-bedded, with bedding attributable to variations in grain sizes.

C3: Colour and the fine grain size are similar to C1. Parts are well-laminated, with bedding horizontal (normal to core elongation).

C4: Ochrous zone continues in only the uppermost 1.5 cm; contact is abrupt against fine-grained, clayey, grey tailings. Except for the contact, which is roughly horizontal, bedding is poorly developed. In the lowermost third of the core, bedding or streaking is parallel to the core elongation axis. Small patches of ochrous material, which occur sporadically and only on the exterior of the core, presumably are contamination.

C5: Again grey and clay-like with poor bedding parallel to the core elongation. Streaks of ochrous material, up to 5 cm long and 1-2 mm wide, occur on the core exterior only, indicating more clearly that this material is a contaminant.

C6: Grey and poorly bedded as in C5, but negligible ochrous contamination. A coarser zone about 2 cm thick near the

Table 2 (cont'd)

bottom of the core indicates that bedding is more likely horizontal than vertical.

C7, C8, C9, C10, C11, C12: Grey, clay-like, with bedding parallel to the core elongation in C7-C10. In C12 the upper half is sandy rather than clayey; apparent bedding is variable from horizontal to vertical.

Table 3. Electron microprobe compositions of carbonates in the Delnite tailings

Sample number		C1T grain 1	C1T grain 2	C1T grain 3	C1T grain 4	C1T grain 5	C1T grain 6	C2T grain 1	C2T grain 2	C2T grain 3	C2T grain 4	C2T grain 5	C2T grain 6
wt%	CaO	28.0	27.8	0.4	27.7	27.6	27.0	0.0	28.3	0.1	29.0	0.1	1.4
	MgO	16.9	17.9	29.3	15.6	16.6	15.1	16.6	17.1	9.9	17.6	14.9	10.6
	FeO	8.0	6.7	22.1	9.4	8.1	10.5	38.5	8.0	46.0	8.0	41.9	45.7
	MnO	0.3	0.4	0.6	0.1	0.4	0.5	0.8	0.5	0.9	0.5	0.8	0.9
	sum	53.2	52.8	52.4	52.8	52.7	53.1	55.9	53.9	56.9	55.1	57.7	58.6
wt%	$CaCO_3$	50.0	49.7	0.2	49.5	49.2	48.2	0.0	50.4	0.2	51.7	0.2	2.5
	$MgCO_3$	35.4	37.5	61.4	32.6	34.7	31.6	34.7	35.7	20.8	36.8	29.1	22.2
	$FeCO_3$	12.9	10.8	35.7	15.1	13.1	17.0	62.0	12.9	74.3	12.9	67.6	73.6
	$MnCO_3$	0.4	0.6	1.0	0.2	0.6	0.8	1.3	0.8	1.5	0.8	1.3	1.5
	ident.	dol.	dol.	mag.	dol.	dol.	dol.	sid.	dol.	sid.	dol.	sid.	sid.

Sample number		C3T grain 1	C3T grain 2	C3T grain 3	C3T grain 4	C3T grain 5	C3T grain 6	C3T grain 7	C3T grain 8	C3T grain 9
wt%	CaO	0.3	28.7	0.3	0.1	28.5	0.1	27.8	0.3	0.4
	MgO	6.8	17.2	8.8	12.8	18.6	10.1	14.9	11.1	8.8
	FeO	49.6	7.7	49.1	43.9	7.6	47.2	10.3	45.1	48.7
	MnO	2.1	0.5	1.0	0.5	0.5	0.5	0.6	1.4	0.9
	sum	58.8	54.1	59.2	57.3	55.2	57.9	53.6	57.9	58.8
wt%	$CaCO_3$	0.5	51.2	0.5	0.2	50.9	0.2	49.7	0.5	0.7
	$MgCO_3$	14.2	36.1	18.4	26.7	38.8	21.2	31.2	23.2	18.4
	$FeCO_3$	80.1	12.4	79.3	70.7	12.3	76.1	16.6	72.8	78.6
	$MnCO_3$	3.3	0.8	1.7	0.8	0.8	0.8	1.0	2.3	1.5
	ident.	sid.	dol.	sid.	sid.	dol.	sid.	dol.	sid.	sid.

Table 4. Electron-microprobe compositions of alteration rims

core	C2-T	C2-T		C2-T		C3-T		
	Fig. 12	Fig. 13, po		Fig. 14, py		Fig. 15, py (+po)		
wt%	po	point 1	point 2	point 1	point 2	point 1	point 2	point 3 (po)
Fe_2O_3	72.2	73.4	74.5	75.5	78.8	72.6	71.1	68.5
CaO	0.0	3.9	3.5	2.4	1.5	3.2	2.5	2.9
SiO_2	2.1	1.7	2.6	2.4	1.7	1.1	1.3	1.3
As_2O_5	5.1	1.5	6.0	2.5	4.0	8.0	8.7	12.9
SO_3	1.7	3.2	2.2	9.5	10.0	3.5	3.0	4.5
sum	81.1	83.7	88.8	92.3	96.0	88.4	86.6	90.1

	C3-T			C3-T	C3-T	
	Fig. 16, po			Fig. 17	Fig. 18, po	
	point 1	point 2	point 3	asp	point 1	point 2
Fe_2O_3	73.8	75.5	66.4	60.6	74.6	73.1
CaO	2.5	2.0	2.8	2.3	2.1	1.4
SiO_2	1.5	1.7	1.9	1.5	1.5	1.7
As_2O_5	9.1	6.6	11.8	18.7	7.2	7.4
SO_3	2.5	2.2	2.2	3.5	3.5	2.2
sum	89.4	88.0	85.1	86.6	88.9	85.8

core	C3-T		C3-T	
	Fig. 19, po		Fig. 20, po	
Fe_2O_3	75.1	74.8	73.8	68.9
CaO	3.2	3.4	3.4	3.1
SiO_2	0.0	0.9	0.9	0.9
As_2O_5	10.0	10.6	10.9	13.0
SO_3	2.7	2.7	2.2	2.5
sum	91.9	92.4	91.2	88.4

po = pyrrhotite; py = pyrite; asp = arsenopyrite

Table 5. Analyses of Delnite pore waters for total cyanide

Site (Fig. 2)	Sample number	Total CN mg/L	Site (Fig. 2)	Sample number	Total CN mg/L
D1	2	2.9	D5	4	0.6
	3	1.8		4A	0.6
	4	0.6		5A	2.2
	5	0.4		5B	2.2
	6	1.0		6A	2.7
D3	2	0.3		6B	2.7
	3	2.1		7	0.8
	4A	<0.1	D17	1	2.1
	4B	<0.1		2	6.2
	4C	<0.1		3	6.0
	5A	1.1		4	2.4
	5B	1.0		5	1.7

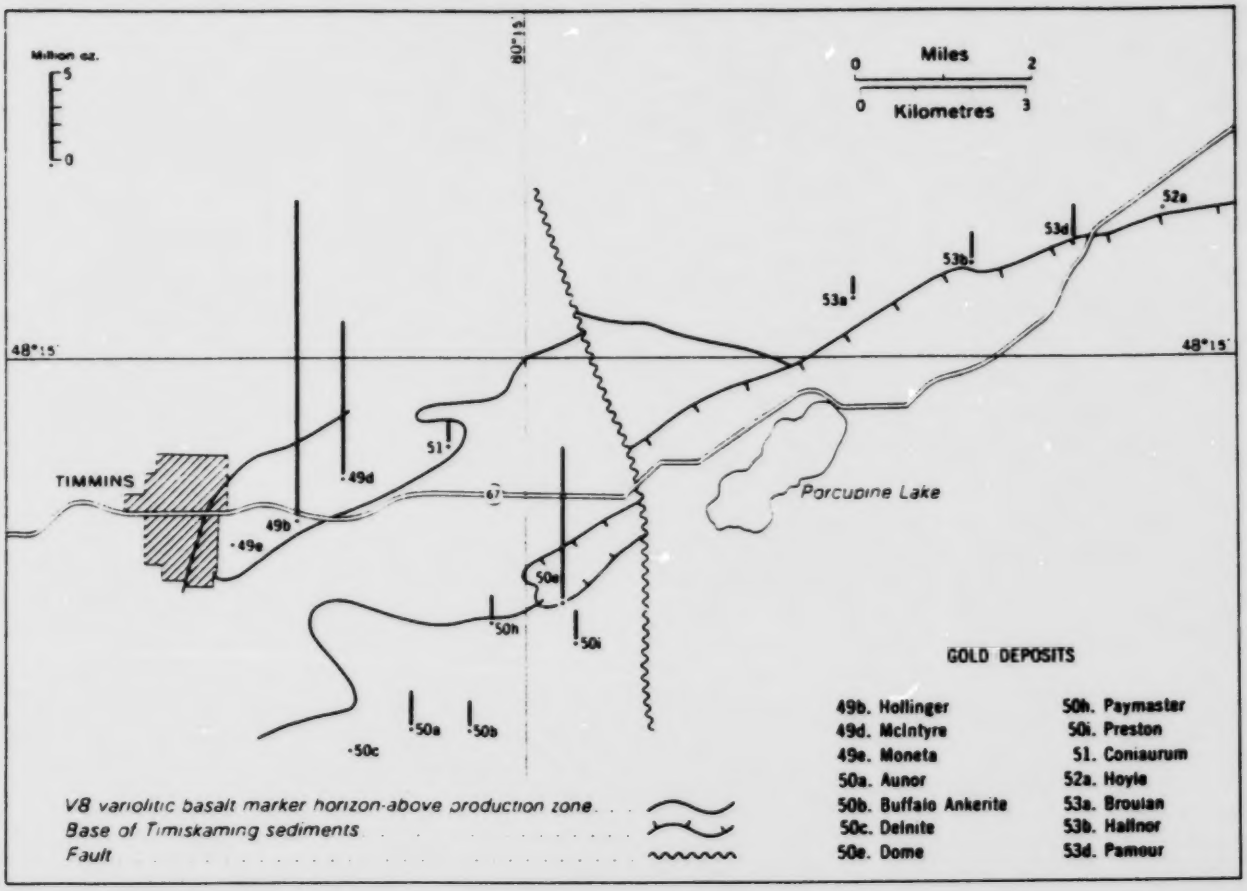

Figure 1. Location, general geological relationship, and relative production of the gold mines in the Timmins area, Ontario (after Douglas 1970).

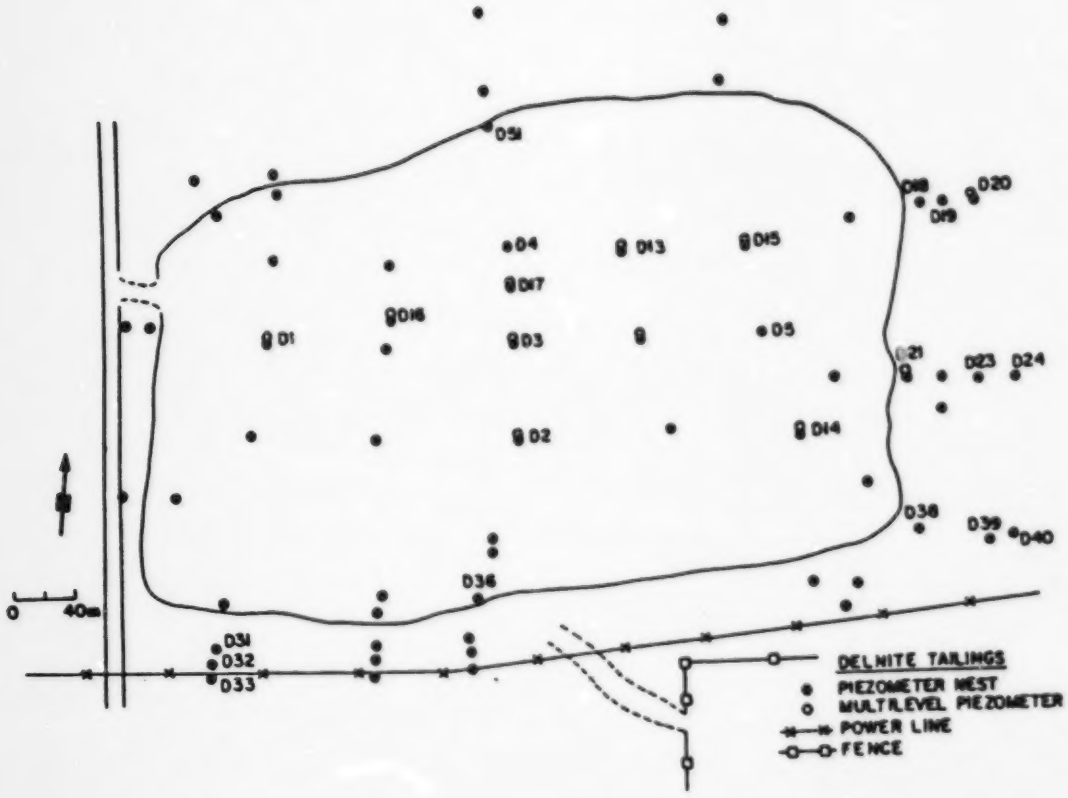

Figure 2. Plan of the Delnite tailings impoundment, showing locations of the piezometer nests. All numbered sites were cored.

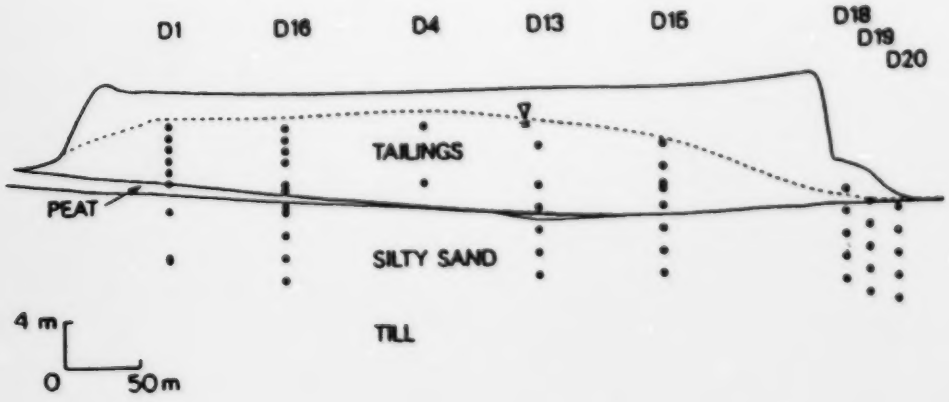

Figure 3. East-west cross-section of Figure 2. Triangle marks the level of the water table.

Figure 4. X-ray diffractograms of core C1-B from hole D1, showing the patterns for sink and float fractions after attempted separation in a heavy liquid of specific gravity 2.89, and after treatment with 5% HCl. Note the disappearance of dolomite (dol) and siderite (sid) in the acid-treated sample. Other abbreviations: ch = chlorite, mu = muscovite, gy = gypsum, tm = tourmaline, q = quartz.

B00513 6/ 1/90 S= 0.050 T=10.000 JAMBOR D-C1B 5%HCL
B00493 5/28/90 S= 0.050 T=10.000 JAMBOR D-C1B S 2.89
B00492 5/28/90 S= 0.050 T=10.000 JAMBOR D-C1B FL 2.89

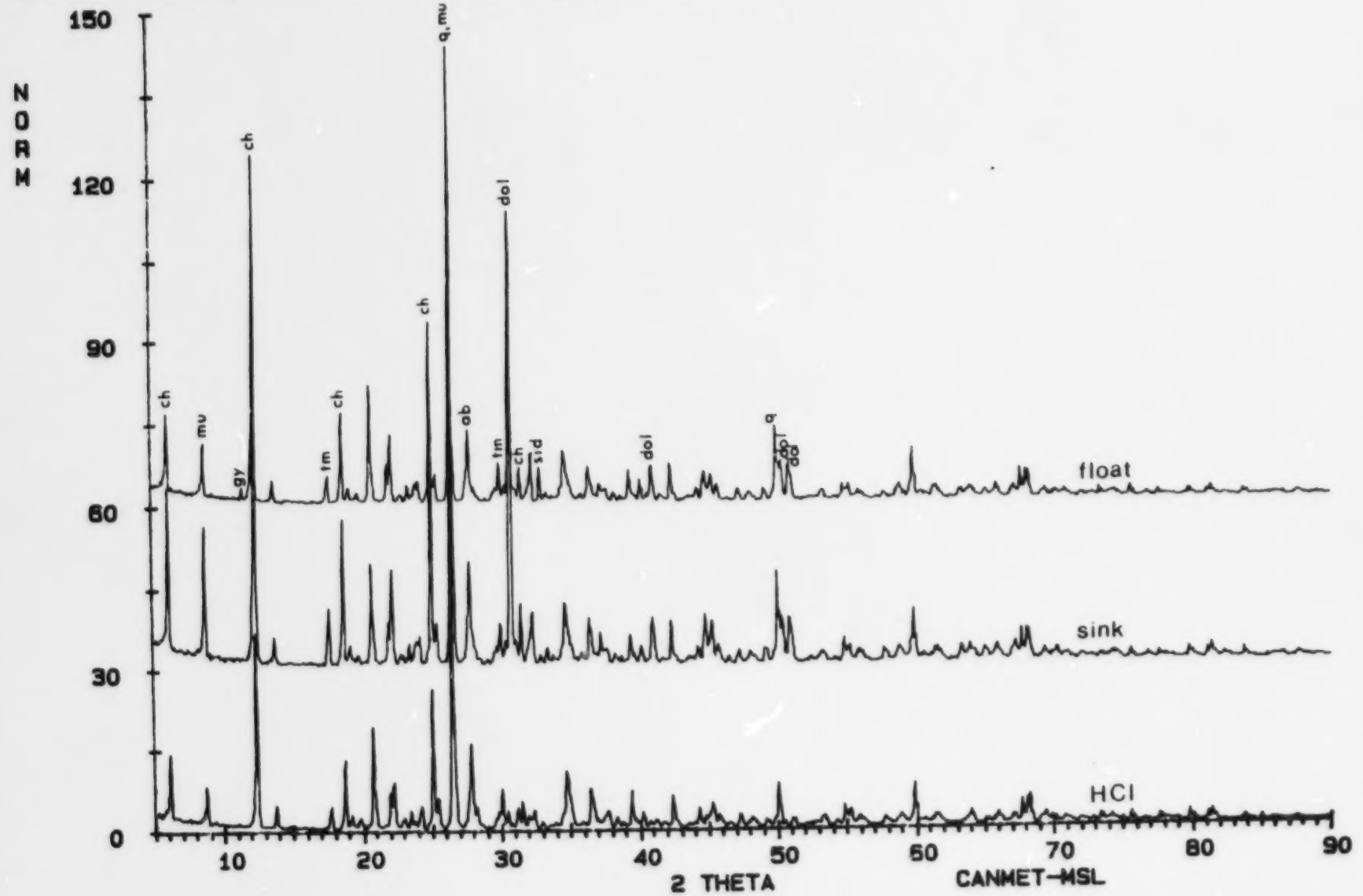

Figure 5. X-ray diffractograms of cores C1, C2, and C3 (T = top, M = middle, and B = bottom of core), hole D1. Abbreviations as in Figure 4, and with ab = albite. Compare with Figure 6.

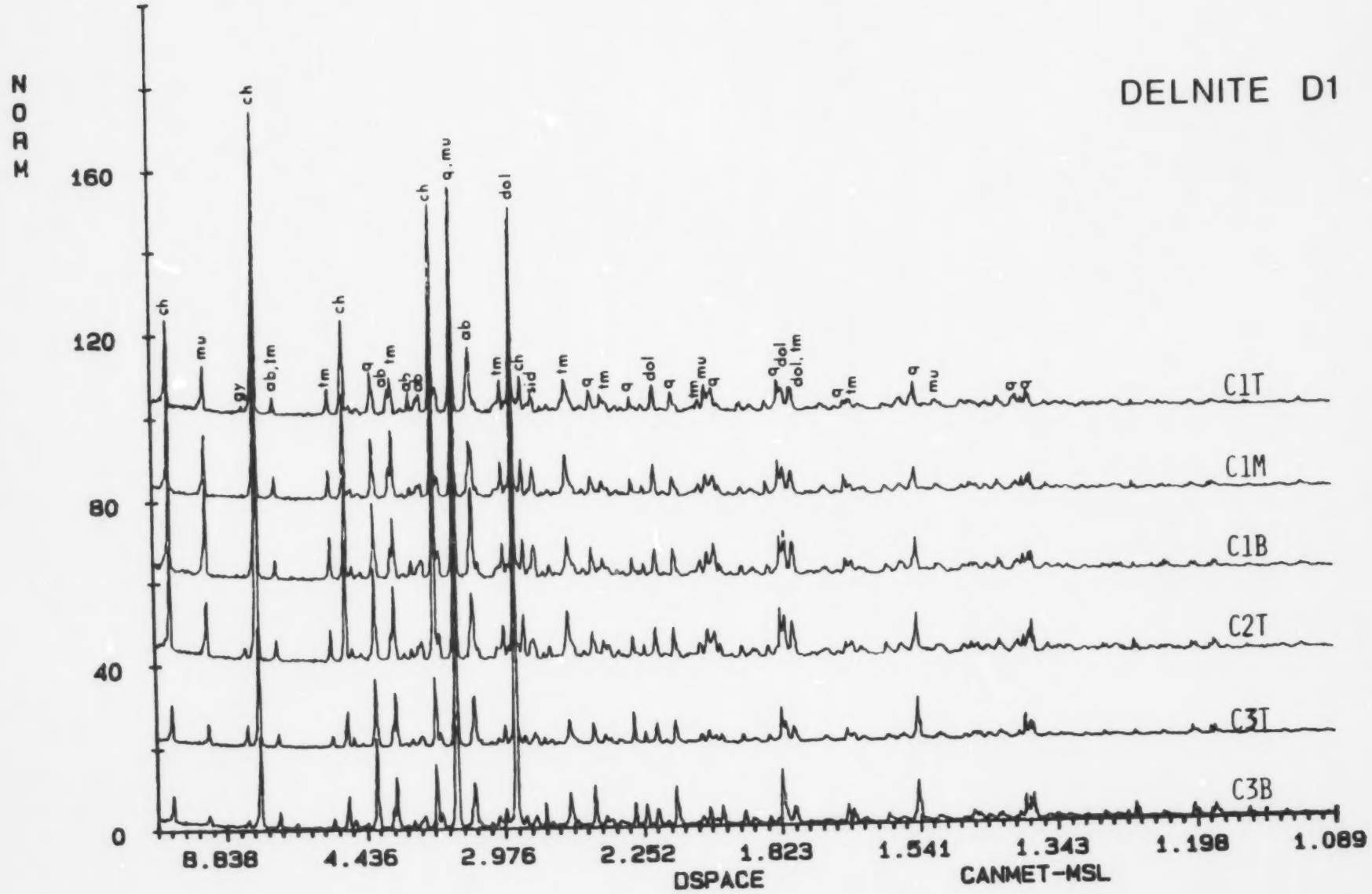
DELNITE D1
NORM
160
120
80
40
0
ch
mu
gy
ab,tm
tm
q
ab
tm
ch
q,mu
ab
dol
tm
ch
sid
tm
q
tm
q
dol
q
tm
mu
q
q
dol
dol,tm
q
tm
q
mu
q
C1T
C1M
C1B
C2T
C3T
C3B
8.838
4.436
2.976
2.252
1.823
1.541
1.343
1.198
1.089
DSPACE
CANMET-MSL

Figure 6. X-ray diffractograms of core samples C4 to C10, hole D1. The most apparent difference is the appearance of talc in this series, and the absence of the gypsum that is evident in Figure 5.

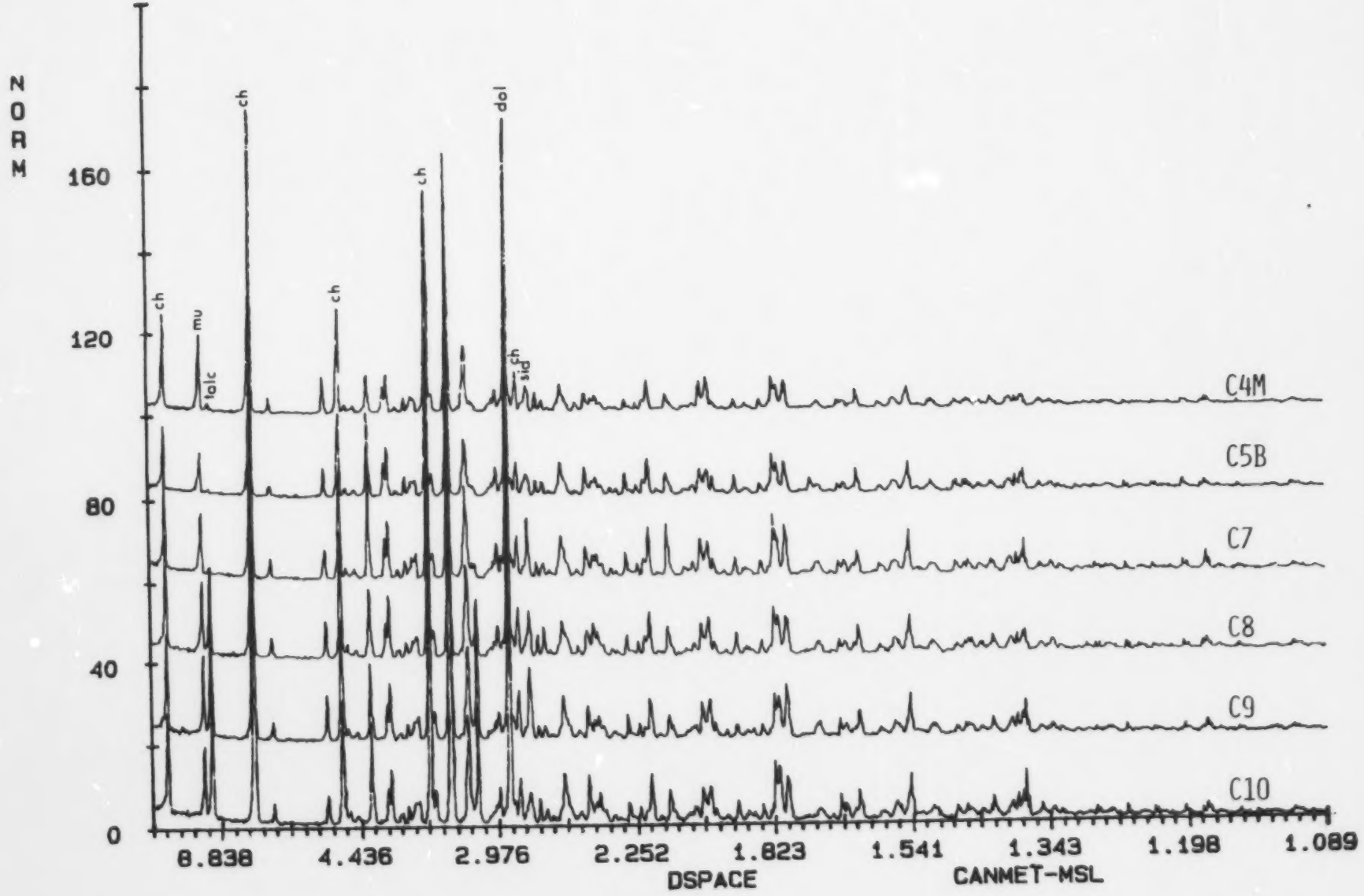
NORM
160
120
80
40
0
ch
mu
talc
ch
ch
dol
ch
sid
C4M
C5B
C7
C8
C9
C10
8.838
4.436
2.976
2.252
1.823
1.541
1.343
1.198
1.089
DSPACE
CANMET-MSL

Figure 7. X-ray diffractograms of cores C1T to C4T, hole D5.

Figure 8. X-ray diffractograms of cores C7 to C12, hole D5. Note that the first appearance of talc is at a depth much greater than that for hole D1.

Figure 9. X-ray diffractograms of cores from hole D5, showing possible depletion of siderite (sid) and dolomite (dol) nearest the surface (C1T), but also showing that carbonate abundance varies from sample to sample.

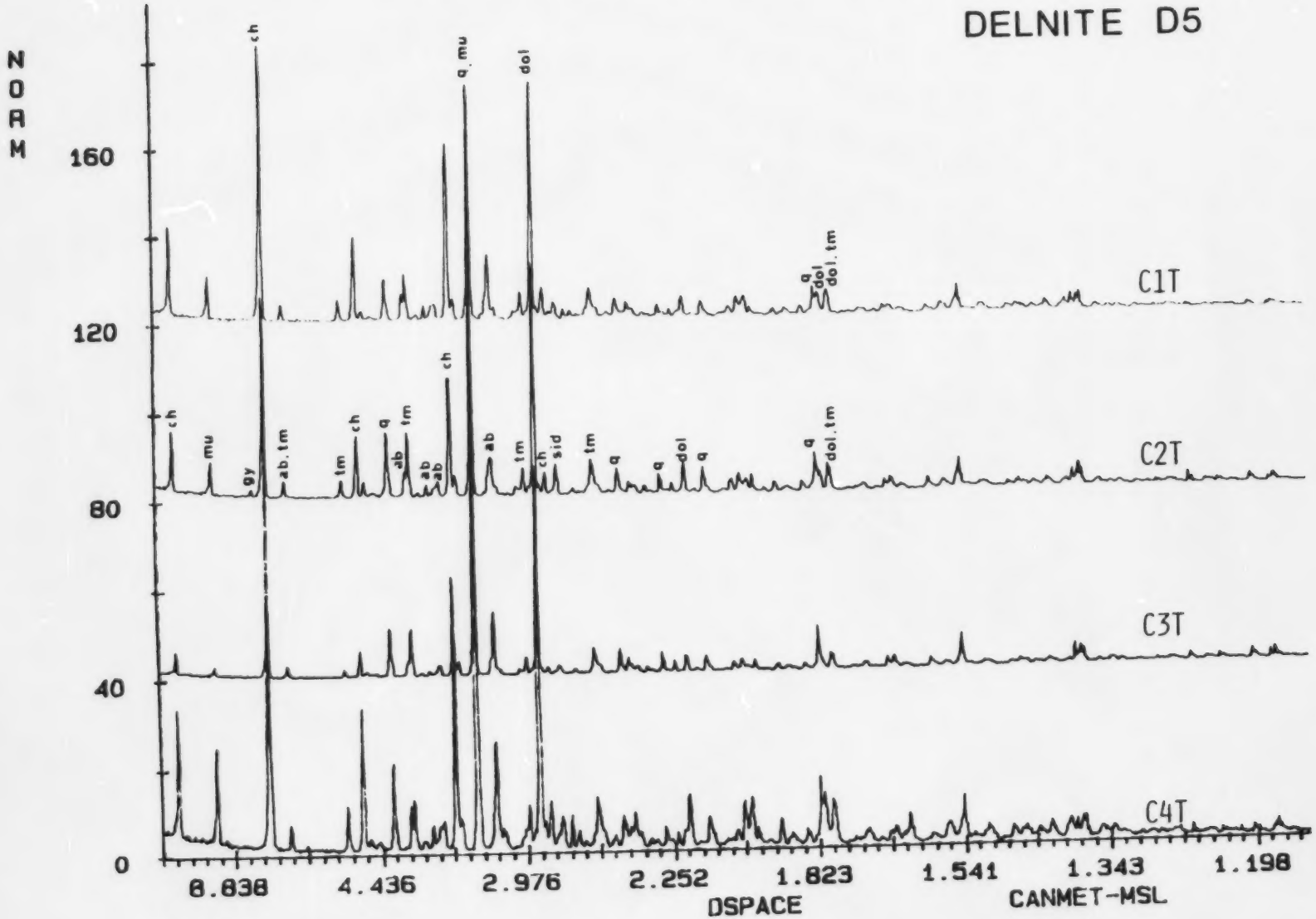
DELNITE D5
NORM
160
120
80
40
0
C1T
C2T
C3T
C4T
ch
q.mu
dol
q
dol
dol.tm
mu
gy
ab.tm
tm
q
ab
sid
8.838
4.436
2.976
2.252
1.823
1.541
1.343
1.198
DSPACE
CANMET-MSL

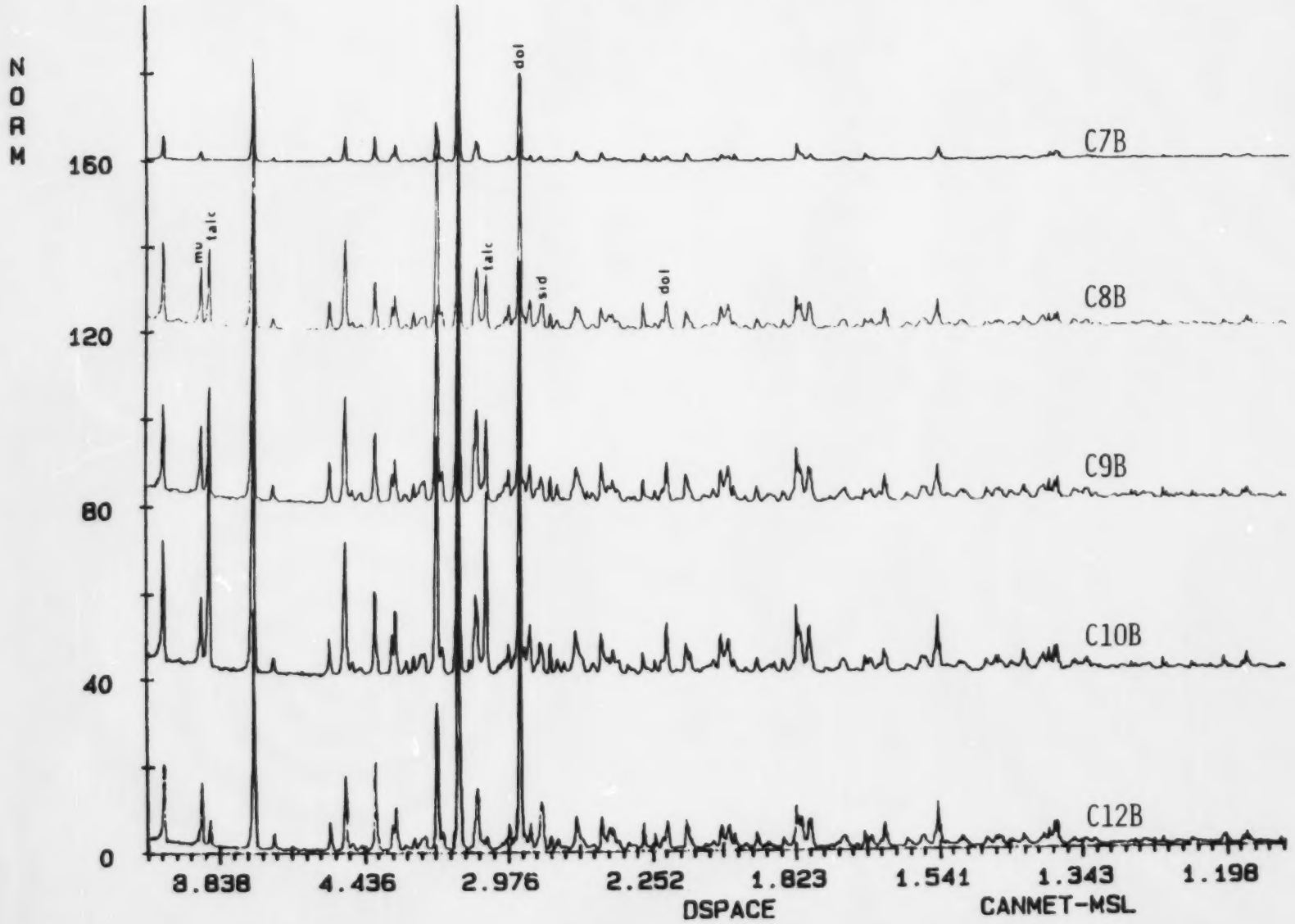
DELNITE D5
NORM
160
120
80
40
0
mu
talc
talc
sid
dol
dol
C7B
C8B
C9B
C10B
C12B
8.838
4.436
2.976
2.252
1.823
1.541
1.343
1.198
DSPACE
CANMET-MSL

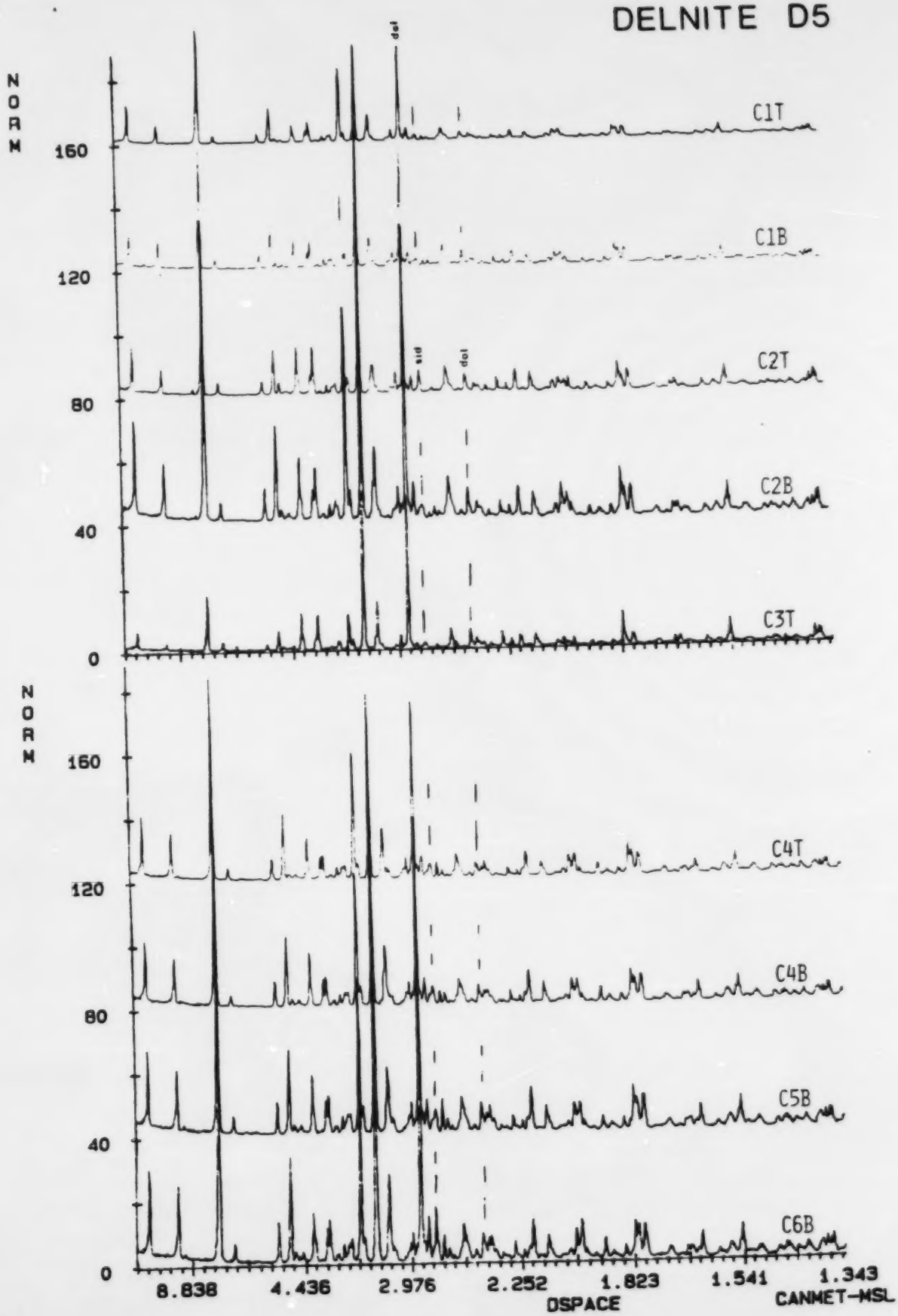
DELNITE D5
NORM
160
120
80
40
0
C1T
C1B
C2T
C2B
C3T
del
sid
del
NORM
160
120
80
40
0
C4T
C4B
C5B
C6B
8.838
4.436
2.976
2.252
1.823
1.541
1.343
DSPACE
CANMET-MSL

Figure 10. Backscattered-electron (BSE) photograph showing hexahydrite ($MgSO_4 \cdot 6H_2O$) as a sphere and as a clear coating formed during the drying of core C5. Bar scale represents 1 µm.

Figure 11. Left photograph (BSE) shows a sphere, probably of native sulphur as indicated by EDX analysis, on the silicate-rich tailings matrix. Right-side photo shows a similar sphere, in which only S and Cl were detected, on a matrix of gypsum. Core C5; bar scales represent 10 µm.

Figures 12-23. Backscattered-electron (BSE) images of sulphide grains surrounded by alteration rims. Accompanying X-ray dot-maps for S(Kα), Fe(Kα), Ca(Kα), As(Lα), and Si(Kα) correspond to the BSE image, and the number of white dots in each photo increases with increased concentration of the specified element. Arrows, and accompanying numbers, correspond to microprobe-analyzed areas for which results are given in Table 4. Unless specified otherwise, the bar scale in all BSE photographs represents 10 μm.

Figure 12. Altered pyrrhotite, core C2-T, hole D1.

Figure 13. Altered pyrrhotite, core C2-T, hole D1.

Figure 14. Alteration rim on pyrite, core C2-T, hole D1. Note that the pyrite is arsenic-bearing (0.7 wt% As by microprobe analysis).

Figure 15. Large grain of residual pyrrhotite (right) accompanied by thinly rimmed pyrite (middle left) and almost completely replaced pyrrhotite (bottom left, analysis area 3).

Figure 16. Residual grain of pyrrhotite, core C3-T, hole D1.

Fe
Si
S
As
I2
Ca

Fe
Si
S
As
13
Ca

Fe
Si
S
As
14
Ca
2

Fe
S
15
2
3
Si
As
Ca

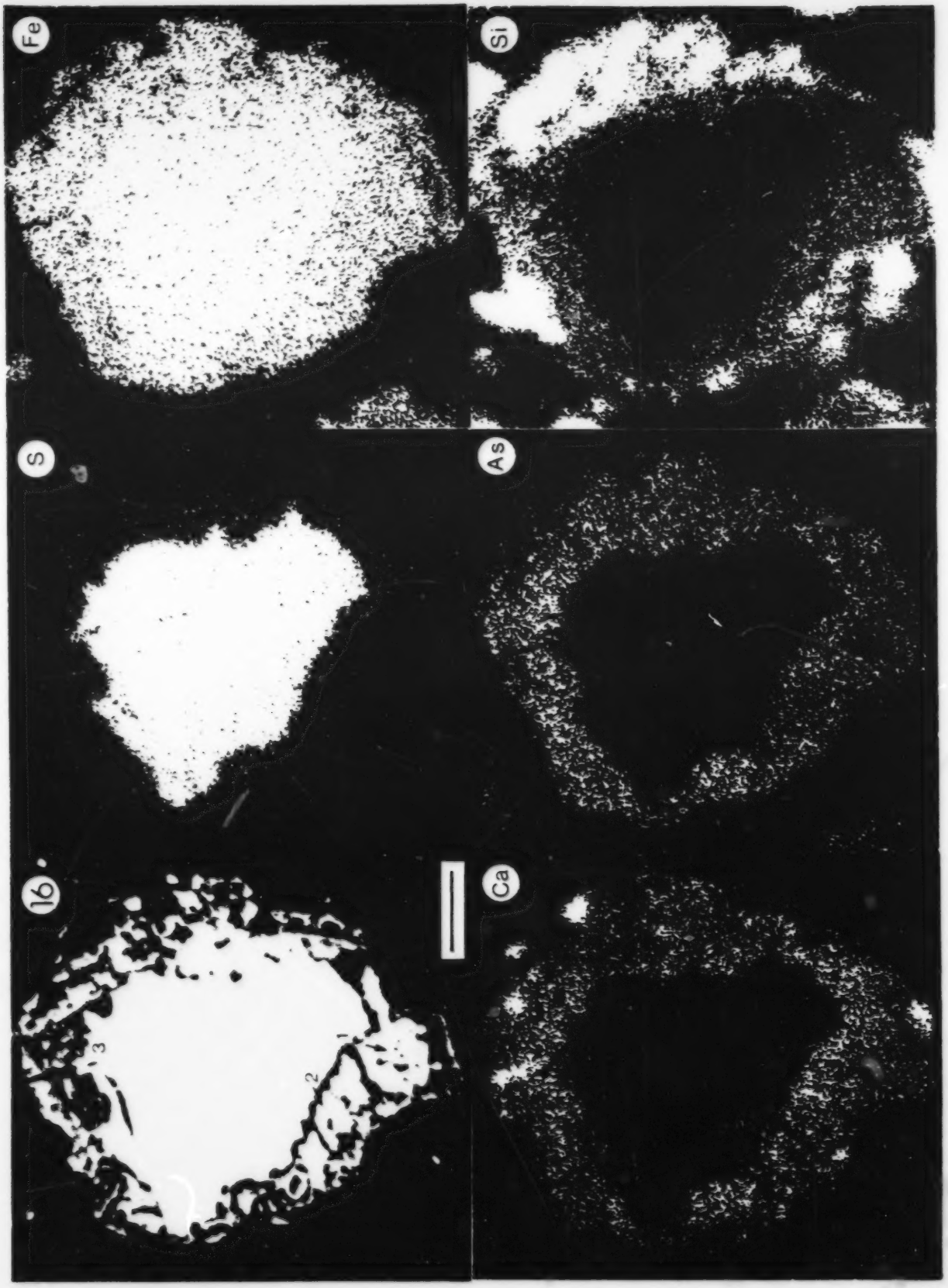
Fe
Si
S
As
16
Ca
3
2
1

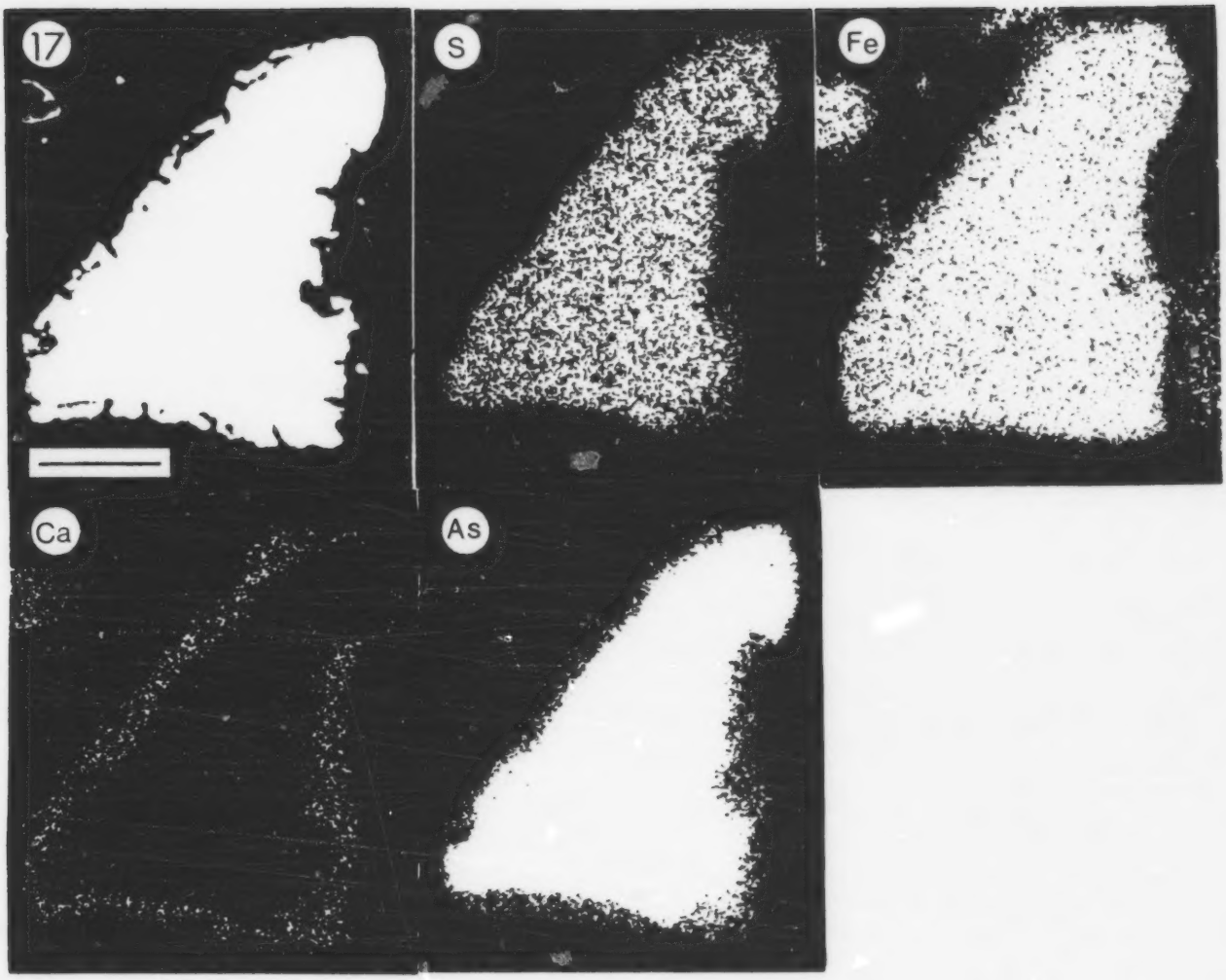

Figure 17. Grain of arsenopyrite, core C3-T, hole D1.

Figure 18. Altered pyrrhotite, accompanied by a smaller grain of less altered pyrite (top). Core C3-T, hole D.

Figure 19. Pyrrhotite with arsenic-rich alteration rim (Table 4). Core C3-T, hole D1.

Figure 20. Pyrrhotite (po), pyrite (py), and arsenopyrite (asp). Alteration rims are arsenic-rich (Table 4). Core C3-T, hole D1.

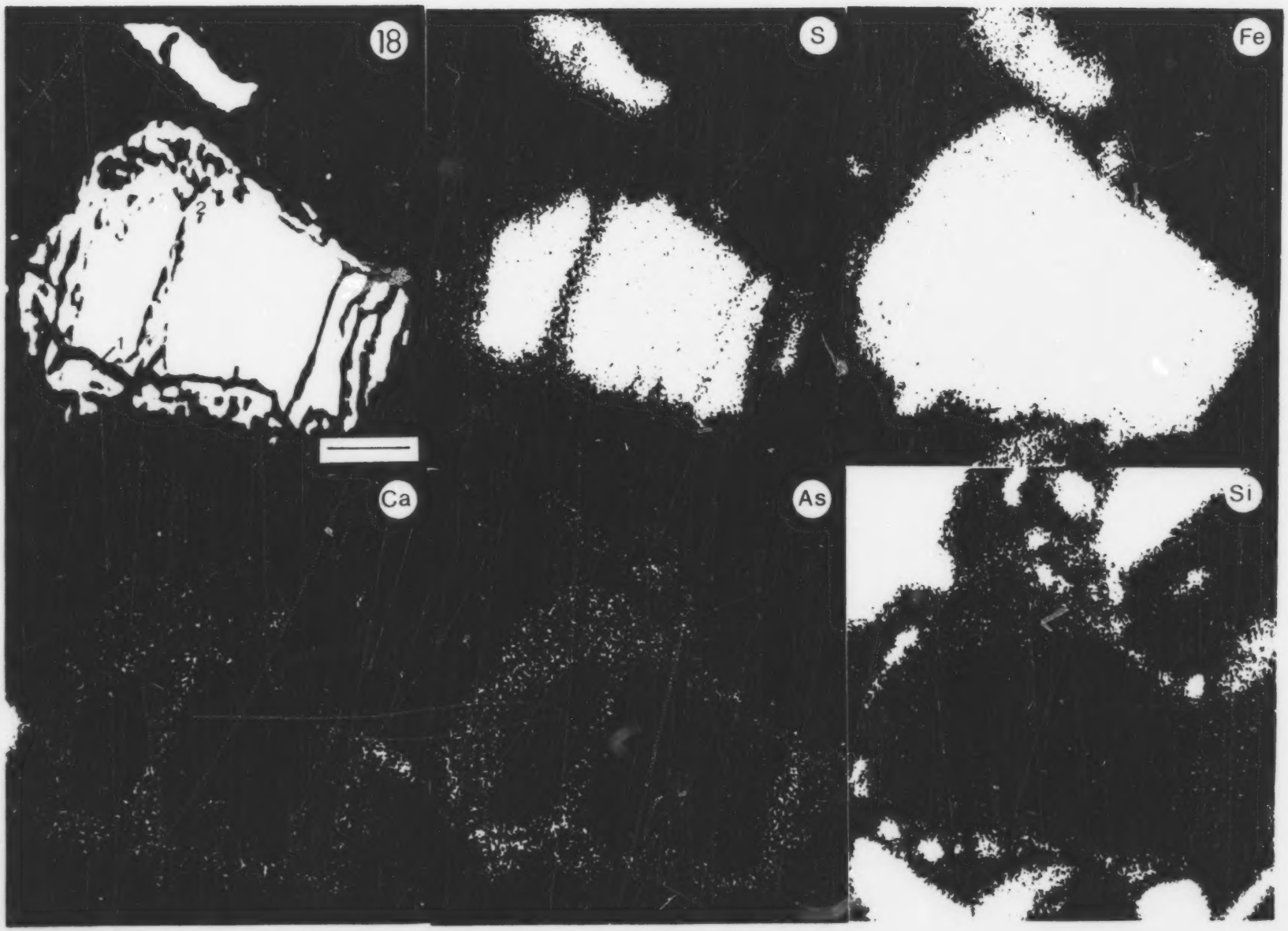
18
1
2
3
Ca
S
Fe
As
Si

19
2
1
S
Fe
Ca
As
Si

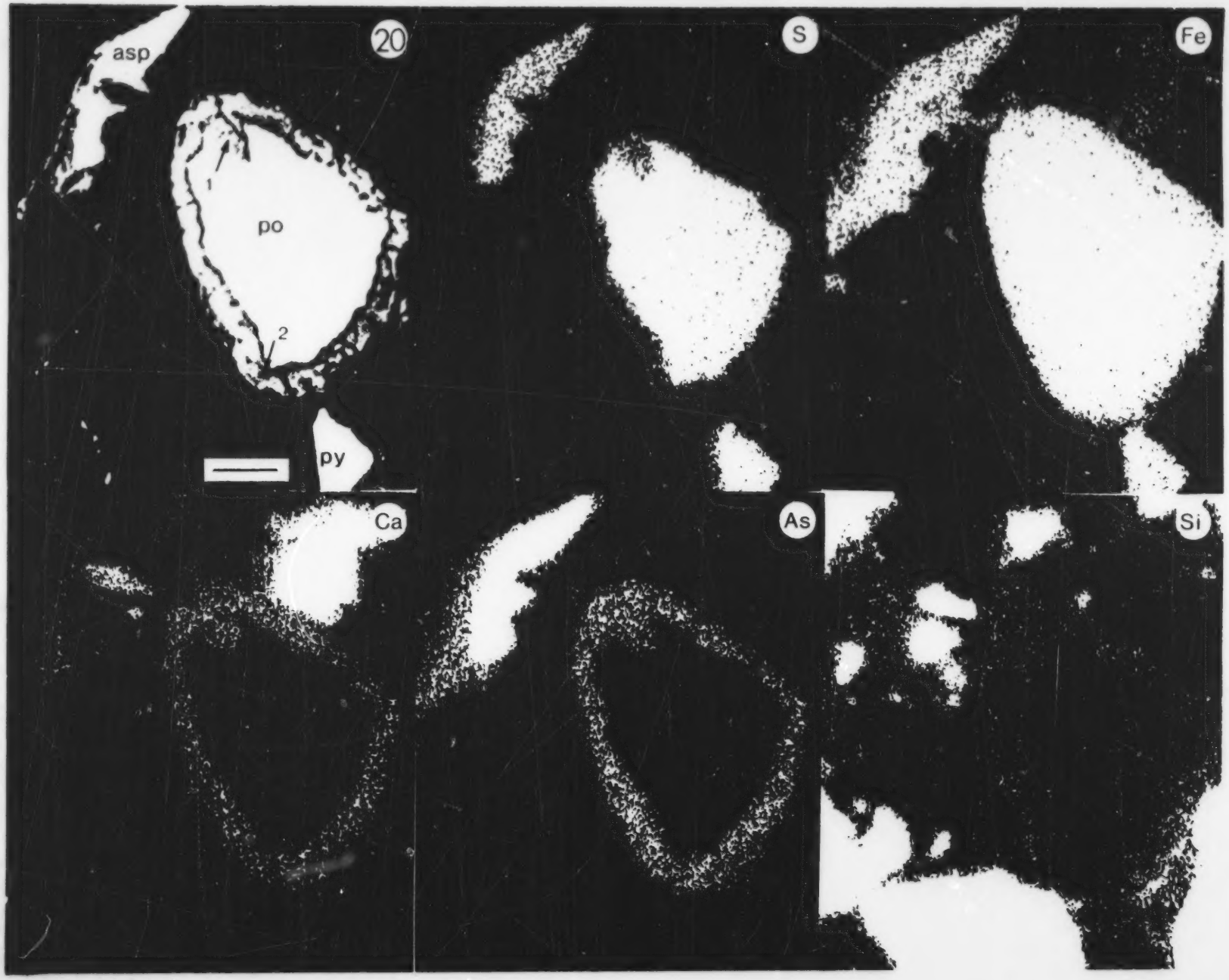
20
asp
1
po
2
py
Ca
S
As
Fe
Si

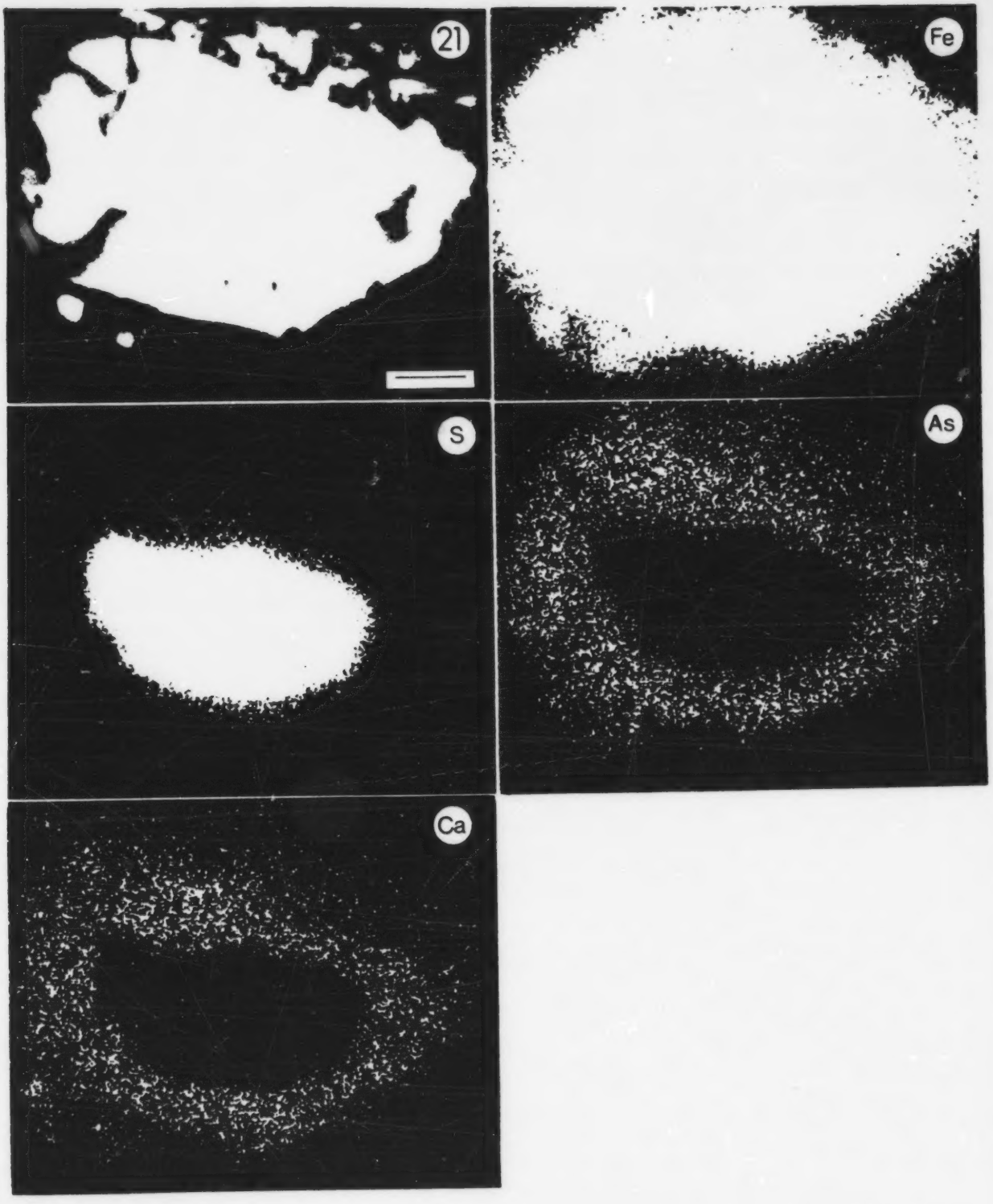

Figure 21. Pyrrhotite remnant surrounded by "goethite" contining As and Ca, but no sulphur. Sample C2T, hole D5. Bar scale represents 5 μm.

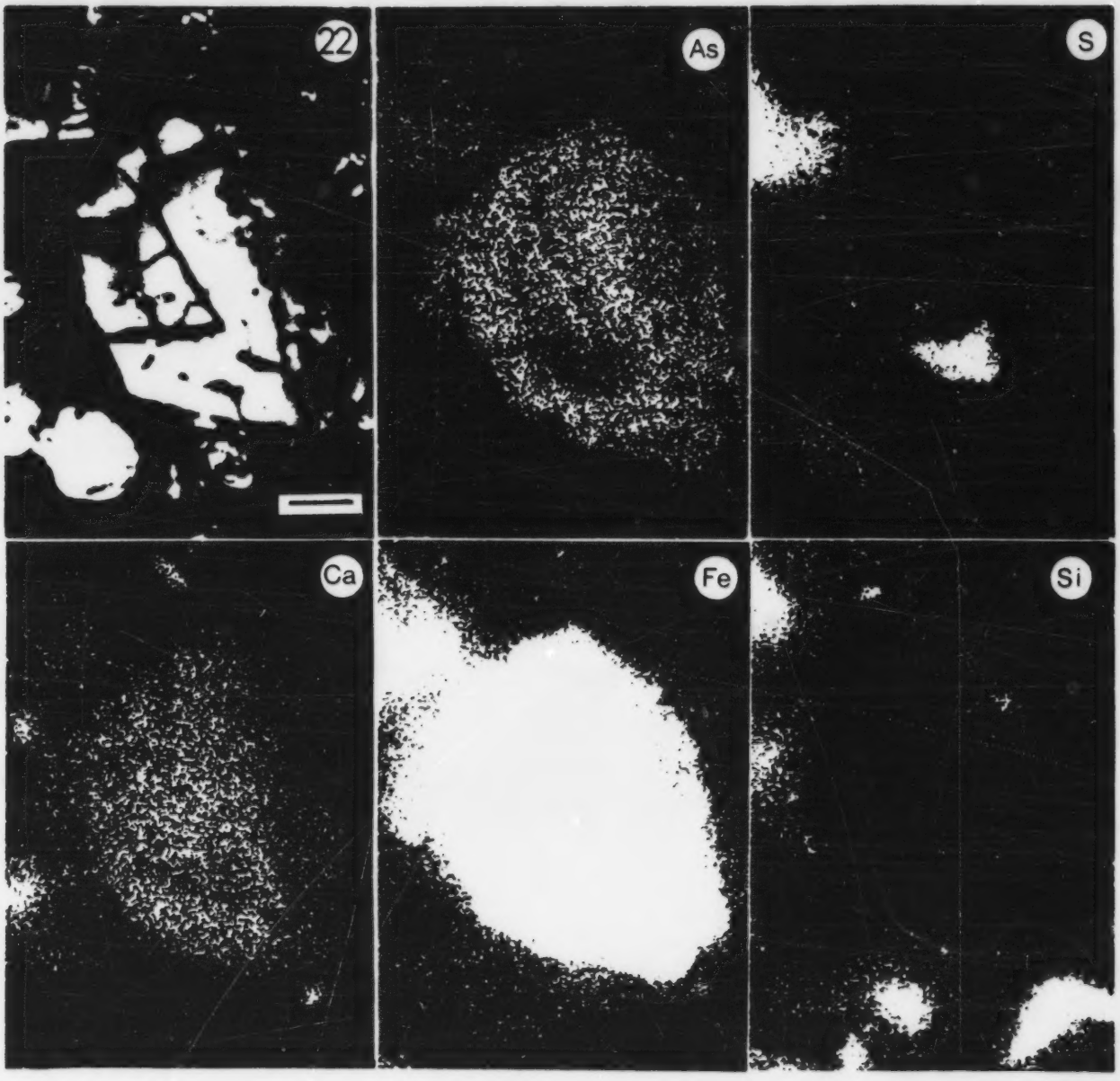

Figure 22. Relict of pyrrhotite in "goethite", sample C2T, hole D5. White, circular areas at bottom left are lap lead. Semiquantitative analysis of the "goethite" gave 2.8% Ca and 6.6% As. Bar scale represents 5 μm.

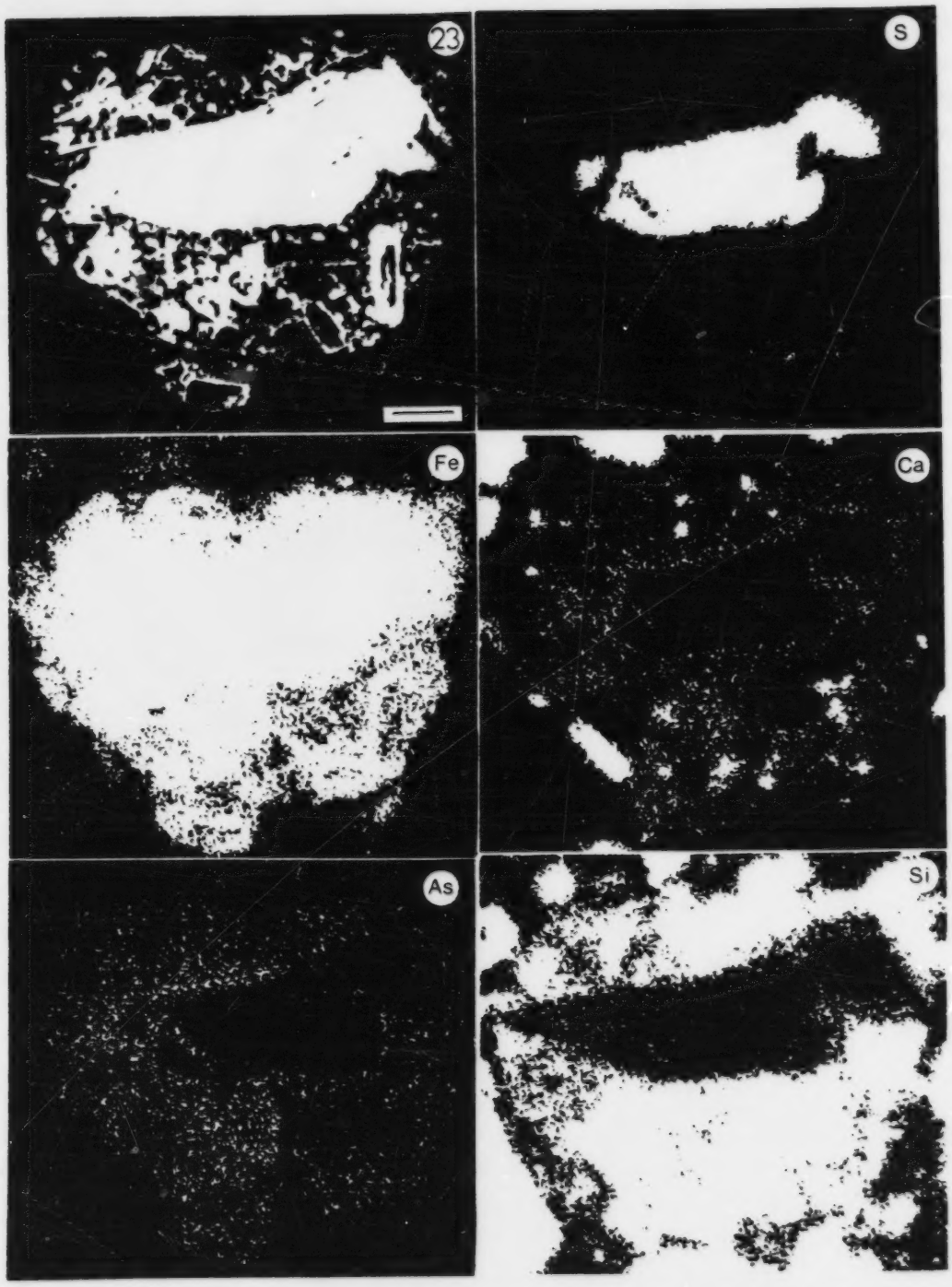

Figure 23. Pyrrhotite remnant (C2T, hole D5) surrounded mainly by silicate and dolomite grains cemented by "goethite" containing Ca and As, but no S.

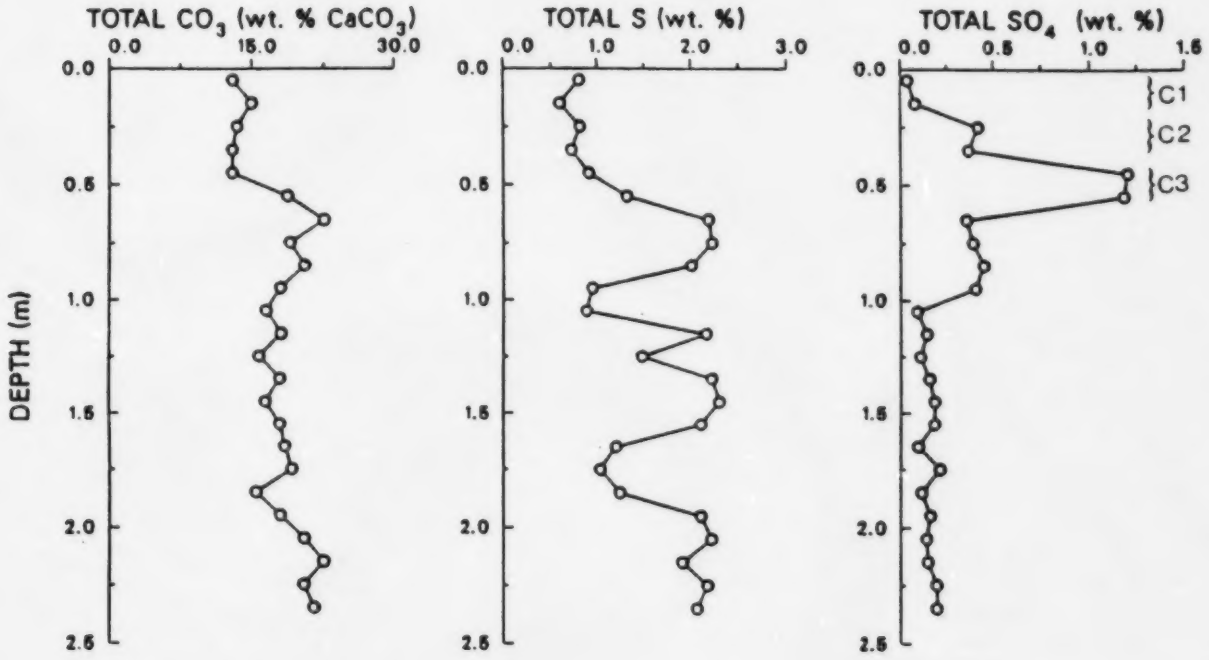

Figure 24. Results of the chemical analyses of tailings solids in Delnite borehole D1 (after Blowes 1990). As is shown in the plot for Total SO_4, sample depths (open circles) correlate with the top and bottom of each of the C-series cores in the present study. Analytical values for CO_3 have been recast as wt% $CaCO_3$.